Electronic Supplementary Material (ESI) for ChemComm.

Supporting Information

Recognition of shorter and longer trimethyllysine analogues by epigenetic reader proteins

Abbas H. K. Al Temimi,[a+] Roman Belle,[a+] Kiran Kumar,[b+] Jordi Poater,[cd+] Peter Betlem,[a+] Bas J. G. E. Pieters,[a] Robert S. Paton,[b] F. Matthias Bickelhaupt[ae] and Jasmin Mecinović*[a]

[a] Institute for Molecules and Materials, Radboud University, Heyendaalseweg 135, 6525 AJ Nijmegen, The Netherlands. E-mail: j.mecinovic@science.ru.nl;
Fax: +31 24 3653393; Tel: +31 24 3652381

[b] Chemistry Research Laboratory, University of Oxford, 12 Mansfield Road, OX1 3TA Oxford, UK.

[c] ICREA, Pg. Lluís Companys 23, 08010 Barcelona, Spain.

[d] Departament de Química Inorgànica i Orgànica & IQTCUB, Universitat de Barcelona, Martí i Franquès 1-11, 08028 Barcelona, Spain.

[e] Department of Theoretical Chemistry and Amsterdam Center for Multiscale Modeling (ACMM), Vrije Universiteit Amsterdam, De Boelelaan 1083, 1081 HV Amsterdam, The Netherlands.

[+] These authors contributed equally to this work

Table of Contents

1. General information

1.1 Methods

^{1}H NMR and ^{13}C NMR spectra were recorded on a Bruker Avance III 500 MHz NMR at 300 K and the chemical shifts are given in parts per million (δ) relative to tetramethylsilane as an internal reference (δ = 0.00 ppm). Coupling constants are reported as *J*-values in Hz. The following abbreviations are used to designate the multiplicities: s = singlet, d = doublet, t = triplet, q = quartet, m = multiplet. High resolution masses were recorded with a JEOL AccuTOF CS JMS-T100CS mass spectrometer. LS-MS analysis for all the compounds was performed on a Thermo Finnigan LCQ-Fleet ESI-ion trap (Thermofischer, Breda, the Netherlands) equipped with a Phenomenex Gemini-NX C18 column, 50 x 2.0 mm, particle size 3 μM (Phenomenex, Utrecht, The Netherlands). An acetonitrile/water gradient containing 0.1 % formic acid was used for elution (5-100 %, 1-50 min, flow 0.2 mL min^{-1}). The room temperature in the reactions is in the range 20-25 ^{o}C. Lyophilization was achieved using an ilShin Freeze Dryer (ilShin, Ede, The Netherlands).

1.2 Materials

All reagents were obtained from commercial sources and used without further purifications. Fmoc-Orn-OH.HCl was purchased from Bachem AG (Bubendorf). Fmoc-hLys(Boc)-OH was purchased from Iris Biotech (Germany). Fmoc amino acid derivatives, N,N'-Disopropylcarbodiimide (DIPCDI), and 1-Hydroxybenzotriazole (HOBt) were obtained from Novabiochem (EMD Chemicals, Gibbstown, USA). Triisopropylsilane (TIS), N,N,-diisopropylethylamine (DIPEA), trifluoroacetic acid (TFA), and piperidine were purchased from Sigma-Aldrich. N,N-dimethylformamide (DMF) solvent for peptide synthesis and gradient degree high-performance liquid chromatography (HPLC) acetonitrile were purchased from Actu-All Chemicals b.v (Oss, The Netherlands).

2. Synthesis of Fmoc amino acids

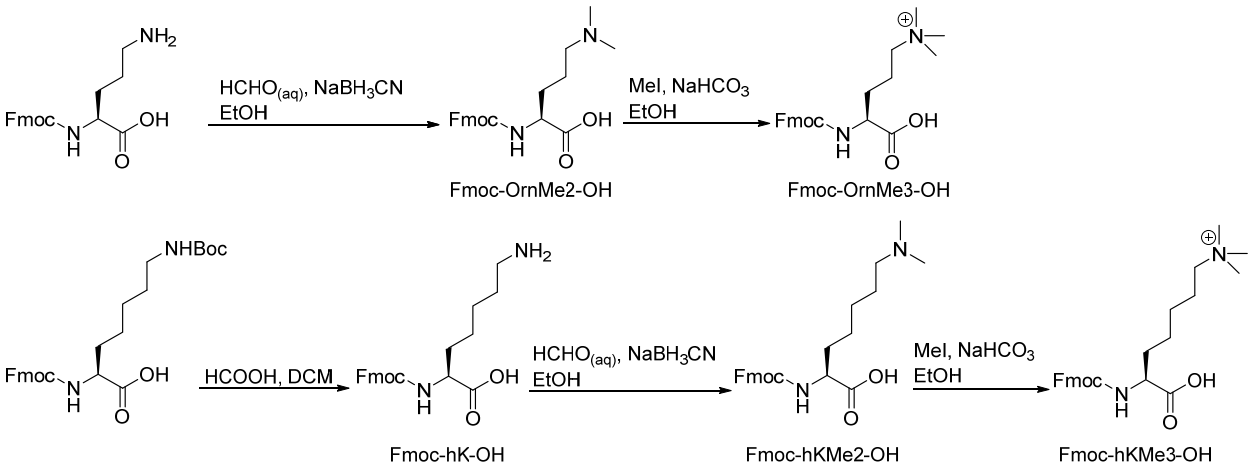

Scheme S1 Synthetic procedures for preparation of Fmoc-OrnMe3-OH and Fmoc-hKMe3-OH.

2.1 Prep-HPLC of the Fmoc amino acids

The crude reaction mixtures of Fmoc amino acids were purified by prep-HPLC on a Shimadzu with a Phenomenex® Gemini-NX 3u C18 110A reversed-phase column (150 x 21.2 mm) using gradient elution at constant flow rate of 10 mL/min and the temperature is 30 °C. A standard run for all the building blocks was carried out using C-18 reverse phase column as shown below. Elution of the target compounds was achieved with water/acetonitrile gradient containing 0.1% trifluoroacetic acid. The pure fractions were combined, frozen, and lyophilised to afford the products. Fmoc-OrnMe2-OH eluted at 13 min, Fmoc-OrnMe3-OH eluted at 13.5 min, Fmoc-hKMe2-OH eluted at 14.5 min, and Fmoc-hKMe3-OH eluted at 15 min.

Time (min)	CH_3CN (%)
1.50	5
2.00	25
14.00	40
14.50	45
15.00	100
29.00	100
30.00	5

(*S*)-2-((((9H-fluoren-9-yl)methoxy)carbonyl)amino)-5-(dimethylamino)pentanoic acid
Fmoc-OrnMe2-OH

To a stirred reaction mixture of Fmoc-Orn-OH.HCl (500.0 mg, 1.3 mmol, 1.0 equiv.) and formaldehyde (232.8 µL, 8.45 mmol, 6.5 equiv) in 5 mL of EtOH was added $NaBH_3CN$ (182.2 mg, 2.9 mmol, 2.2 equiv.) in portions. The reaction was then left to stir for 4.5 h at room temperature, after which 1 mL of TFA was added to the mixture and the solvent was evaporated *in vacuo* to obtain colorless oil. The crude product was redissolved in MeOH, filtered through syringe filter, and purified by prep-HPLC system to obtain pure colorless oil for use in solid phase peptide synthesis. ^{1}H NMR (500 MHz, CD_3OD) δ 7.82 (d, *J* = 7.5 Hz, 2H), 7.69 (dd, *J* = 10.1, 7.6 Hz, 2H), 7.41 (t, *J* = 7.5 Hz, 2H), 7.33 (t, *J* = 7.4 Hz, 2H), 4.45 (dd, *J* = 10.6, 6.7 Hz, 1H), 4.37 (dd, *J* = 10.6, 6.9 Hz, 1H), 4.24 (dt, *J* = 10.4, 5.7 Hz, 2H), 3.21 – 3.11 (m, 2H), 2.88 (d, *J* = 2.4 Hz, 6H), 1.98 – 1.93 (m, 1H), 1.88 – 1.73 (m, 3H); ^{13}C NMR (126 MHz, CD_3OD) δ 173.5, 157.3, 143.9, 141.2, 127.4, 126.8, 124.7, 119.6, 66.6, 56.9, 53.1, 47.0, 42.1, 28.1, 20.9. HRMS $[M+H]^+$ calculated 383.1971, found 383.1966.

(*S*)-4-((((9H-fluoren-9-yl)methoxy)carbonyl)amino)-4-carboxy-N,N,N-trimethylbutan-1 aminium
Fmoc-OrnMe3-OH

To a stirred solution of Fmoc-OrnMe2-OH (200.0 mg, 0.52 mmol, 1.0 equiv.) in EtOH (2 mL) were added $NaHCO_3$ (109.2 mg, 1.3 mmol, 2.5 equiv.) and MeI (329.5 µL, 5.2 mmol, 10.0 equiv.). The reaction mixture was stirred at room temperature for 3 days. Additional amounts of MeI (329.5 µL) and $NaHCO_3$ (109.2 mg) were required to drive the reaction to the completion. The progress of the reaction was monitored by LC-MS. Volatiles were then evaporated, and the remaining crude product was redissolved in MeOH, filtered through syringe filter, and purified by prep-HPLC system to obtain pure colorless oil for use in solid phase peptide synthesis. ^{1}H NMR (500 MHz, CD_3OD) δ 7.83 (d, *J* = 7.5 Hz, 2H), 7.70 (dd, *J* = 11.8, 7.5 Hz, 2H), 7.42 (t, *J* = 7.5 Hz, 2H), 7.34 (tt, *J* = 7.4, 1.3 Hz, 2H), 4.48 (dd, *J* = 10.6, 6.7 Hz, 1H), 4.38 (dd, *J* = 10.6, 6.9 Hz, 1H), 4.30 – 4.22 (m, 2H), 3.45 – 3.34 (m, 2H), 3.12 (s, 9H), 2.09 – 1.86 (m, 3H), 1.80 – 1.76 (m, 1H); ^{13}C NMR (126 MHz, CD_3OD) 157.4, 143.9, 141.2, 127.4, 126.8, 124.7, 119.6, 66.6, 65.6, 52.1, 47.0, 42.1, 28.1, 19.2. HRMS $[M+H]^+$ calculated 397.2127, found 397.2134.

(*S*)-2-((((9H-fluoren-9-yl)methoxy)carbonyl)amino)-7-aminoheptanoic acid Fmoc-hK-OH

Fmoc-hK(Boc)-OH (500 mg, 1.04 mmol, 1.0 equiv.) was dissolved in formic acid (5 mL) and DCM (5 mL), and the reaction mixture was then stirred at room temperature for 3 h. The volatiles were then removed *in vacuo*. The residual oil was coevaporated with Et_2O (5 mL, 2×), PhMe (5 mL, 2×), and $CHCl_3$ (5 mL, 2×) to afford a white solid. ^{1}H NMR (500 MHz, CD_3OD) δ 7.82 (d, *J* = 7.5 Hz, 2H), 7.69 (dd, *J* = 10.0, 7.5 Hz, 2H), 7.41 (t, *J* = 7.5 Hz, 2H), 7.33 (td, *J* = 7.5, 1.1 Hz, 2H), 4.44 – 4.32 (m, 2H), 4.25 (t, *J* = 7.0 Hz, 1H), 4.18 (dd, *J* = 9.3, 4.8 Hz, 1H), 2.93 (t, *J* = 7.6 Hz, 2H), 1.89 (ddd, *J* = 15.2, 7.7, 4.9 Hz, 1H), 1.79 – 1.61 (m, 3H), 1.54 – 1.26 (m, 4H); ^{13}C NMR (126 MHz, CD_3OD) δ 174.4, 157.4, 143.9, 141.2, 127.4, 126.8, 124.8, 119.5, 66.6, 53.6, 47.0, 39.2, 31.0, 27.0, 25.4, 25.0. HRMS $[M+H]^+$ calculated 383.1971, found 383.1975.

(*S*)-2-((((9H-fluoren-9-yl)methoxy)carbonyl)amino)-7-(dimethylamino)heptanoic acid Fmoc-hKMe2-OH

To a suspension of Fmoc-hK-OH (380.0 mg, 0.91 mmol, 1.0 equiv.) in EtOH (5 mL) was added formaldehyde (157.9 μL, 5.7 mmol, 6.3 equiv.). $NaBH_3CN$ (124.9 mg, 2.0 mmol, 2.2 equiv.) was predissolved in EtOH (5 mL) and the solution was then added to the stirred reaction mixture. The mixture was left to stir at room temperature for 5 h, then TFA (1 mL) was added, and the volatiles were evaporated *in vacuo*. The remaining crude product was re-dissolved in MeOH, filtered through syringe filter, and purified by prep-HPLC system to obtain pure colorless oil for use in solid phase peptide synthesis. ^{1}H NMR (500 MHz, CD_3OD) δ 7.82 (d, *J* = 7.5 Hz, 2H), 7.70 (dd, *J* = 10.3, 7.5 Hz, 2H), 7.41 (t, *J* = 7.4 Hz, 2H), 7.33 (td, *J* = 7.5, 1.1 Hz, 2H), 4.41 (dd, *J* = 10.6, 7.0 Hz, 1H), 4.35 (dd, *J* = 10.5, 7.0 Hz, 1H), 4.25 (t, *J* = 7.0 Hz, 1H), 4.18 (dd, *J* = 9.4, 4.8 Hz, 1H), 3.14 – 3.08 (m, 2H), 2.87 (s, 6H), 1.95 – 1.83 (m, 1H), 1.79 – 1.65 (m, 3H), 1.55 – 1.28 (m, 4H); ^{13}C NMR (126 MHz, CD_3OD) δ 174.4, 157.3, 143.9, 141.2, 127.4, 126.8, 124.8, 119.5, 66.6, 57.5, 53.6, 47.0, 42.0, 31.0, 25.4, 25.0, 24.0. HRMS $[M+H]^+$ calculated 411.2284, found 411.2289.

(S)-6-((((9H-fluoren-9-yl)methoxy)carbonyl)amino)-6-carboxy-N,N,N-trimethylhexan-1-aminium

Fmoc-hKMe3-OH

To a stirred solution of Fmoc-hKMe2-OH (200.0 mg, 0.49 mmol, 1.0 equiv.) in EtOH (2 mL) were added $NaHCO_3$ (102.9 mg, 1.23 mmol, 2.5 equiv.) and MeI (308.4 μL, 4.86 mmol, 10.0 equiv.). After 1 day, additional amounts of MeI (308.4 μL) and $NaHCO_3$ (102.9 mg) were added, and the reaction mixture was stirred at room temperature for another 2 days. Volatiles were then evaporated, and the remaining crude product was redissolved in MeOH, filtered through syringe filter, and purified by prep-HPLC system to obtain pure colorless oil for use in solid phase peptide synthesis. ^{1}H NMR (500 MHz, CD_3OD) δ 7.82 (d, *J* = 7.5 Hz, 2H), 7.70 (dd, *J* = 10.6, 7.5 Hz, 2H), 7.42 (t, *J* = 7.5 Hz, 2H), 7.33 (td, *J* = 7.5, 1.2 Hz, 2H), 4.42 (dd, *J* = 10.5, 6.9 Hz, 1H), 4.35 (ddd, *J* = 10.5, 7.0, 3.0 Hz, 1H), 4.25 (t, *J* = 7.0 Hz, 1H), 4.18 (dd, *J* = 9.4, 4.7 Hz, 1H), 3.34-3.31 (m, 2H), 3.12 (s, 9H), 1.92 (tdd, *J* = 13.8, 8.1, 4.1 Hz, 1H), 1.86 – 1.68 (m, 2H), 1.48 (m, 2H), 1.35 – 1.27 (m, 1H); ^{13}C NMR (126 MHz, CD_3OD) δ 174.4, 157.3, 143.9, 141.2, 127.4, 126.8, 124.9, 119.5, 66.6, 66.3, 53.6, 52.1, 47,0, 31.0, 25.3, 25.0, 22.3. HRMS $[M+H]^+$ calculated 425.2440, found 425.2438.

2.2 NMR spectra

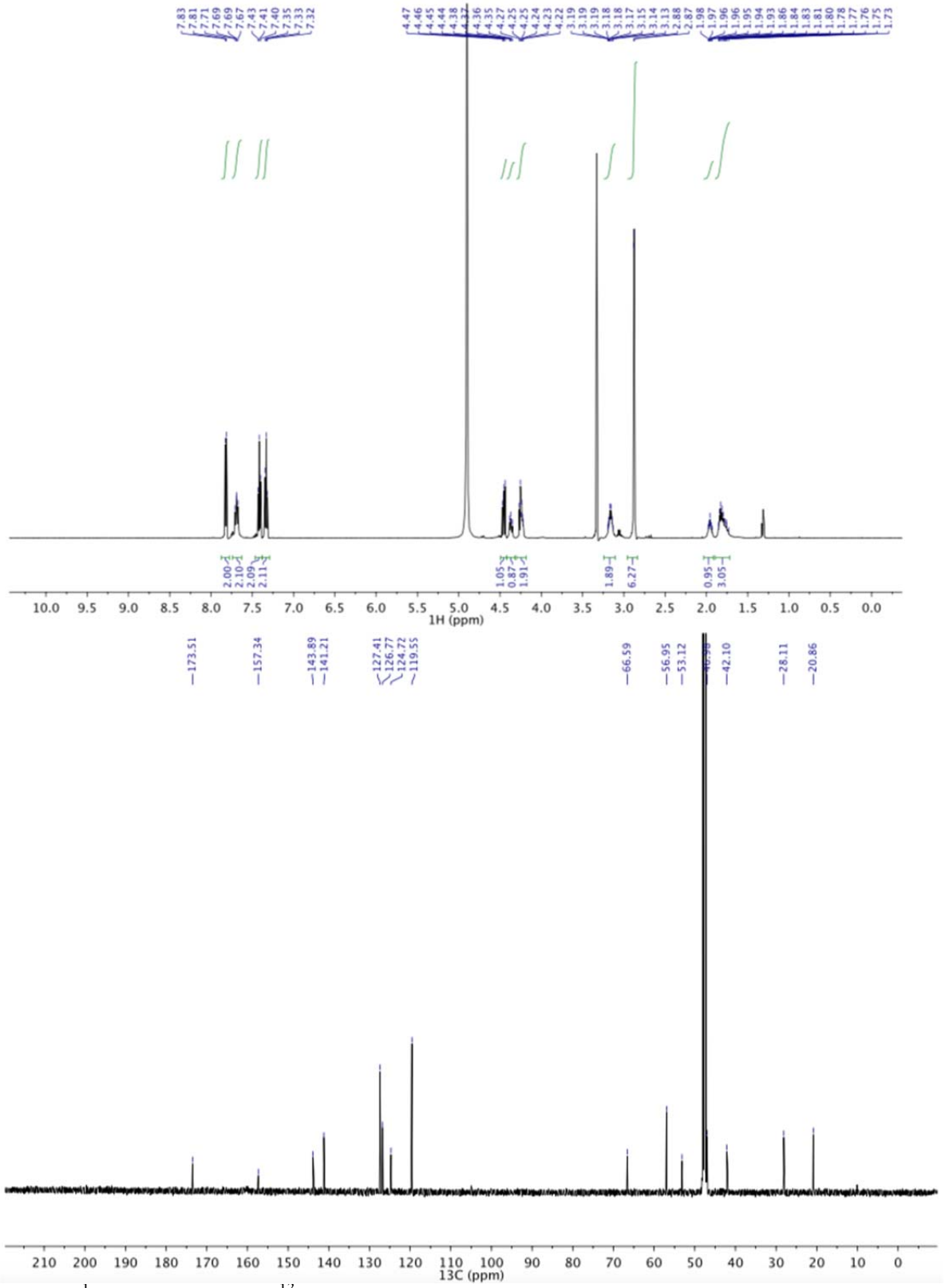

Fig. S1 ^{1}H NMR (top) and ^{13}C NMR (bottom) spectra of Fmoc-OrnMe2-OH.

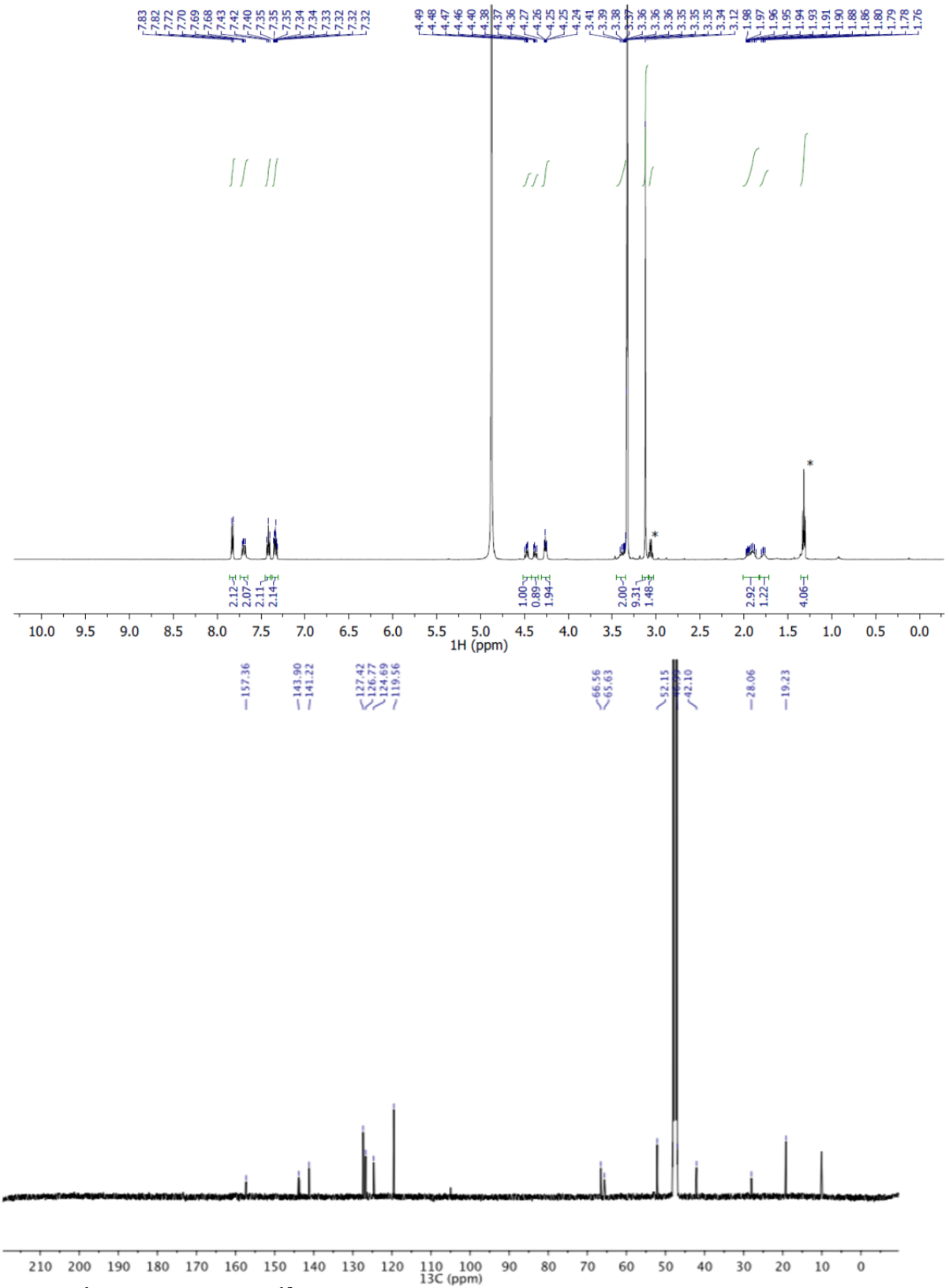

Fig. S2 ^{1}H NMR (top) and ^{13}C NMR (bottom) spectra of Fmoc-OrnMe3-OH. * shows impurities.

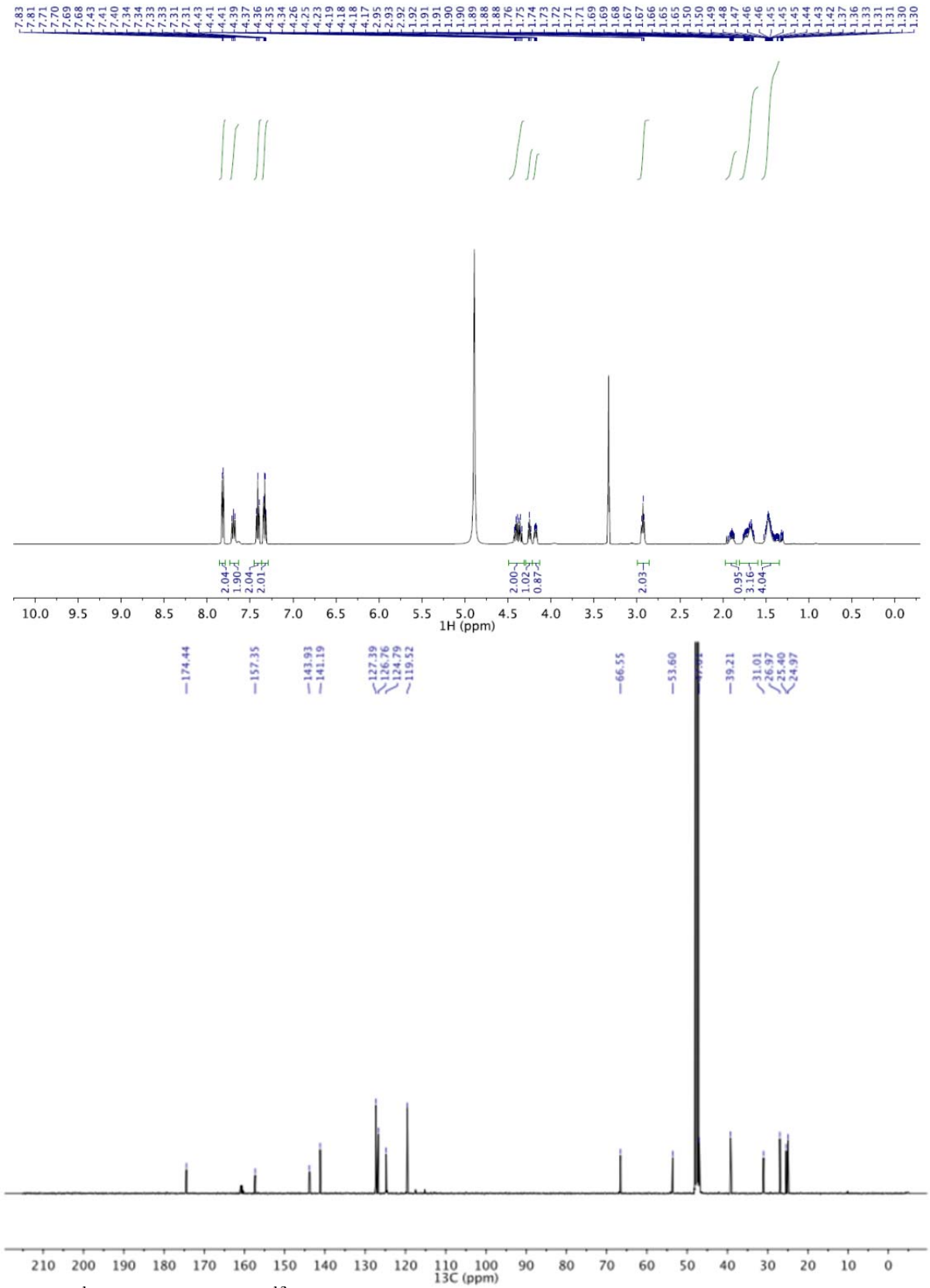

Fig. S3 ^{1}H NMR (top) and ^{13}C NMR (bottom) spectra of Fmoc-hK-OH.

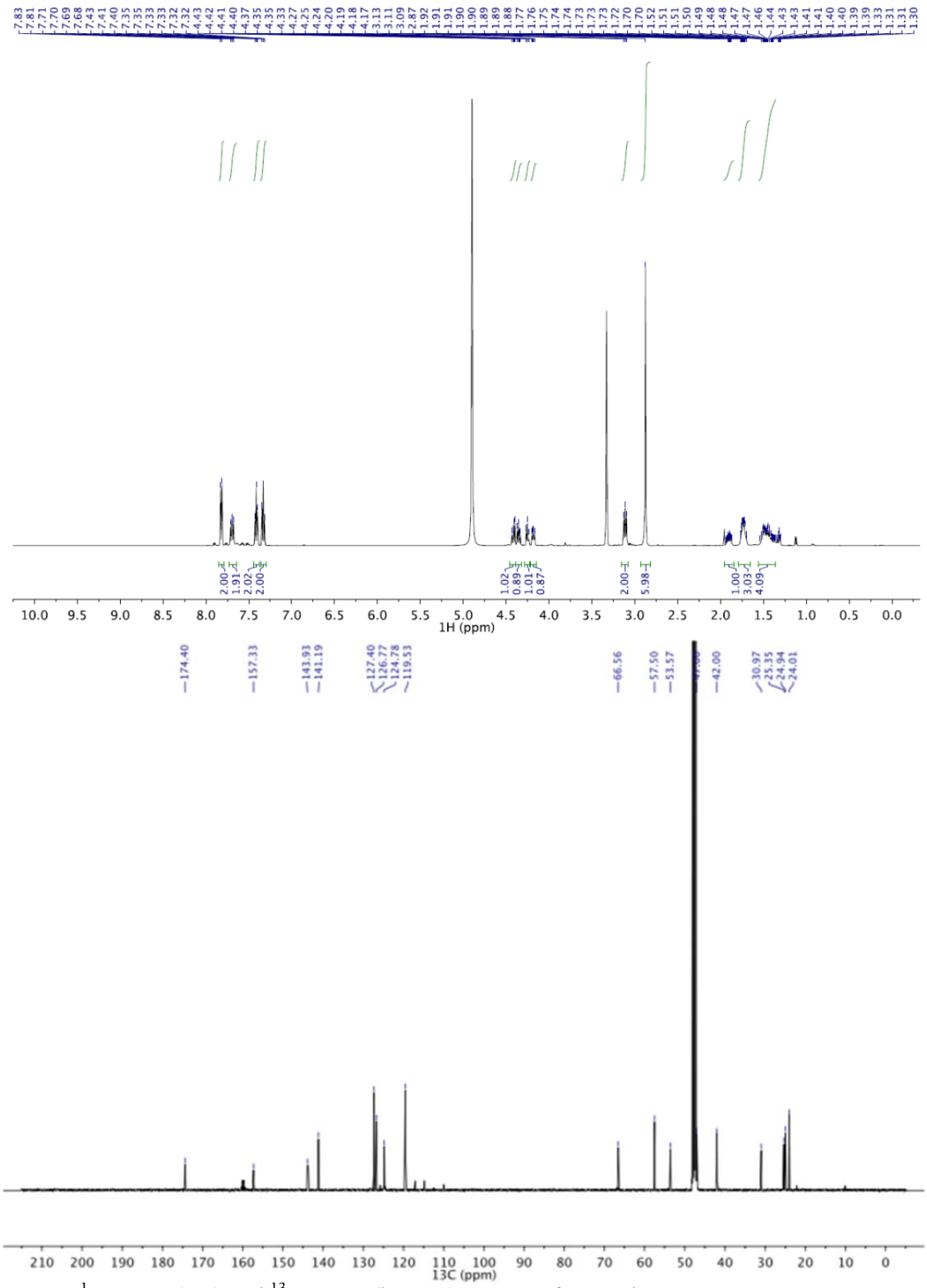

Fig. S4 ^{1}H NMR (top) and ^{13}C NMR (bottom) spectra of Fmoc-hKMe2-OH.

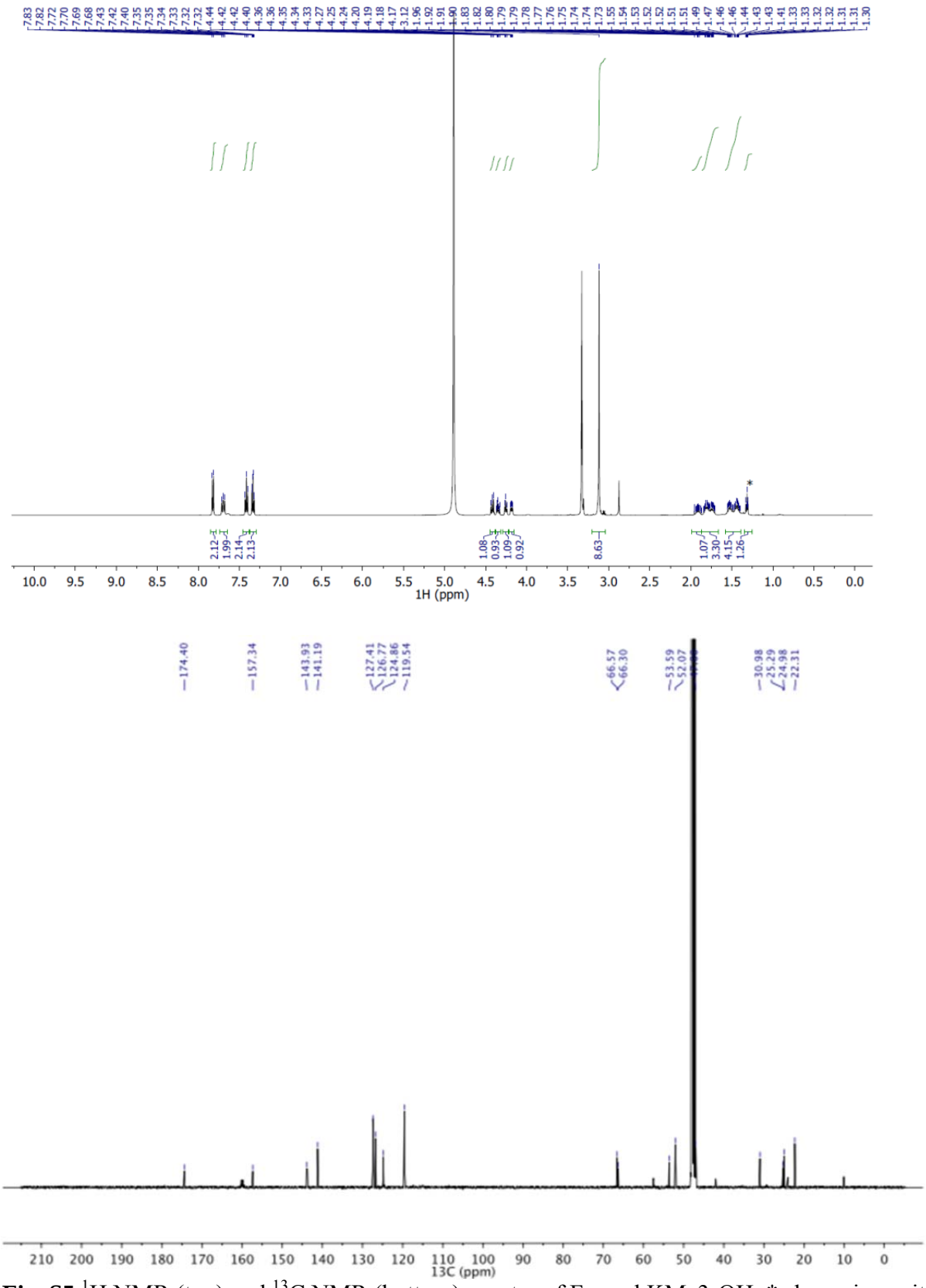

Fig. S5 ^{1}H NMR (top) and ^{13}C NMR (bottom) spectra of Fmoc-hKMe3-OH. * shows impurities.

3. Synthesis and purification of histone peptides

3.1 Solid Phase Peptide Synthesis

The synthesis of the required 10-mer histone peptides was achieved manually by standard Fmoc solid phase peptide synthesis (SPPS) using a cartridge (15 mL, 20 µm, Screening Devices B.V., The Netherlands). Synthesis was done on 0.15 mmol scale and loaded with Wang resin (0.5 mmol/g). Side chain protection was as follows: Arg(Pbf), Thr(tBu), Gln(Trt), Lys(Boc), and Ser(tBu). Coupling conditions were 3.0 equivalents of the amino acid, 3.6 equivalents coupling reagent 1M HOBt in DMF, and 3.3 equivalents of 1M DIPCDI in DMF. The latter components were premixed for 2 min and were added to the resin. The mixture was shaken for 1 h at room temperature to ensure efficient coupling. Fmoc-OrnMe3-OH and Fmoc-hKMe3-OH were incorporated into position 4 with elongated reaction time of 16 h at room temperature. The Fmoc protection group was removed by agitation with 20% piperidine in DMF for 30 min. The coupling reactions and Fmoc deprotections were monitored with the colour Kaiser test. All amino acid couplings was examined with the pre-Kaiser test after 1 h before washing with DMF to avoid any possible side products due to incomplete amino acid couplings. After deprotection of the last Fmoc group, the solid support was removed by incubating the peptidyl-resin with a mixture of TFA/TIS/H_2O (95:2.5:2.5) for 4 h at room temperature. The resulted crude peptide was precipitated in cold diethyl ether (-20 °C), after which it was recovered by centrifugation at 4,000 rpm for 5 min at +4 °C (3×). The residual ether was removed by evaporation and the crude peptides purified by preparative HPLC using the same method as previously described.[1, 2] The purity and the identity of the obtained peptide were confirmed by analytical HPLC and ESI-MS.

3.2 Analytical HPLC of histone peptides

The Analytic HPLC of the natural and unnatural 10-mer histone peptides was performed on a Shimadzu LC-2010A HPLC system (Shimadzu, Kyoto, Japan) on RP C18 column from Phenomenex, Prodigy ODS3, particle size 5 µm, pore size 110 Å, length 150 mm, and internal diameter 4.60 mm. The analysis was performed using solvent gradient of acetonitrile and water (both solvents containing 0.1% TFA) at flow rate 10 mL/min. After 1 min at 5% a gradient of 5% to 100% over 30 min was introduced, followed by 5 min at 100% to 100%. Finally, the system was allowed to re-equilibrate for 14 min. The HPLC signal was recorded at 214 nm absorbance. The retention time of each peptide was shown on the top of the corresponding peak in HPLC chromatogram. The used MilliQ water was purified using a WaterPro PS Polisher (Labconco), set to 18.2 MΩ/cm.

3.3 Chromatogram of purified histone peptides

A)

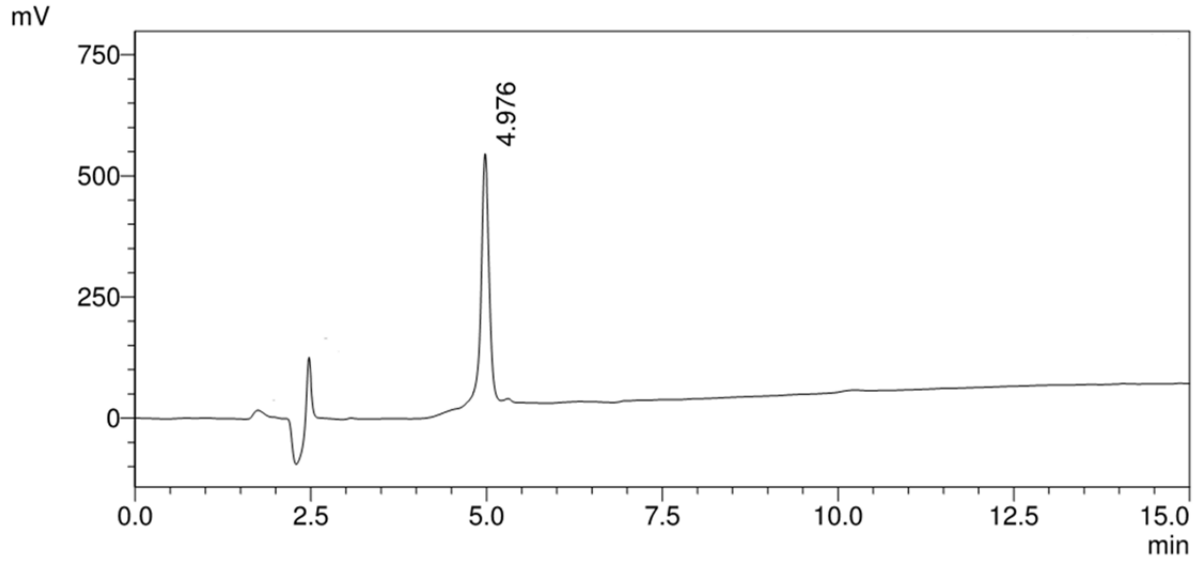

B)

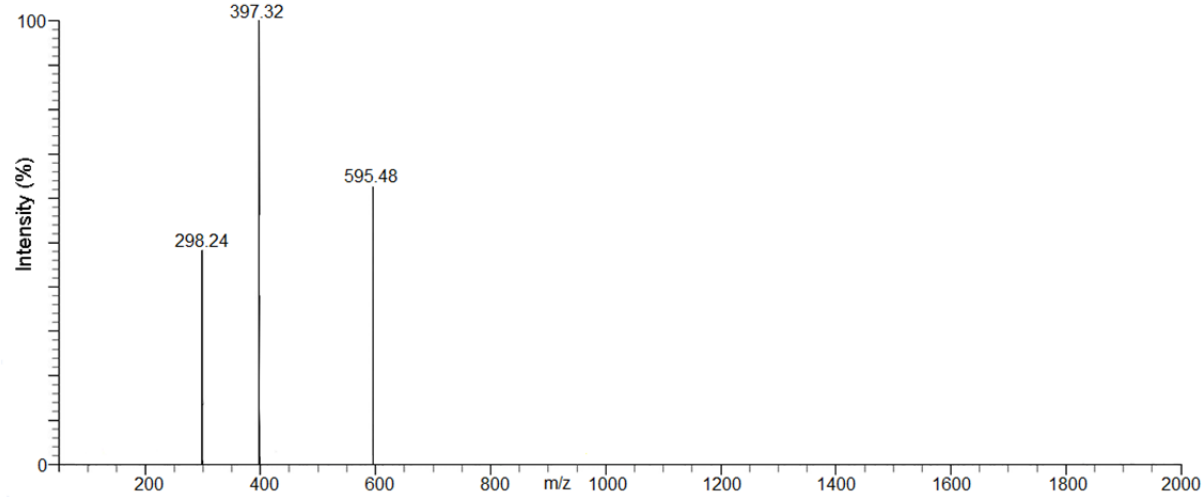

Fig. S6 (A) Analytical HPLC profile and **(B)** ESI-MS analysis of H3K4Me3 peptide after prep-HPLC purification. The peptide elutes at 4.9 min. Calculated mass as $[M+H]^{+}$: 1189.4 Da, observed: 595.48 $[M+2H]^{2+}$, 397.32 $[M+3H]^{3+}$, 298.24 $[M+4H]^{4+}$.

A)

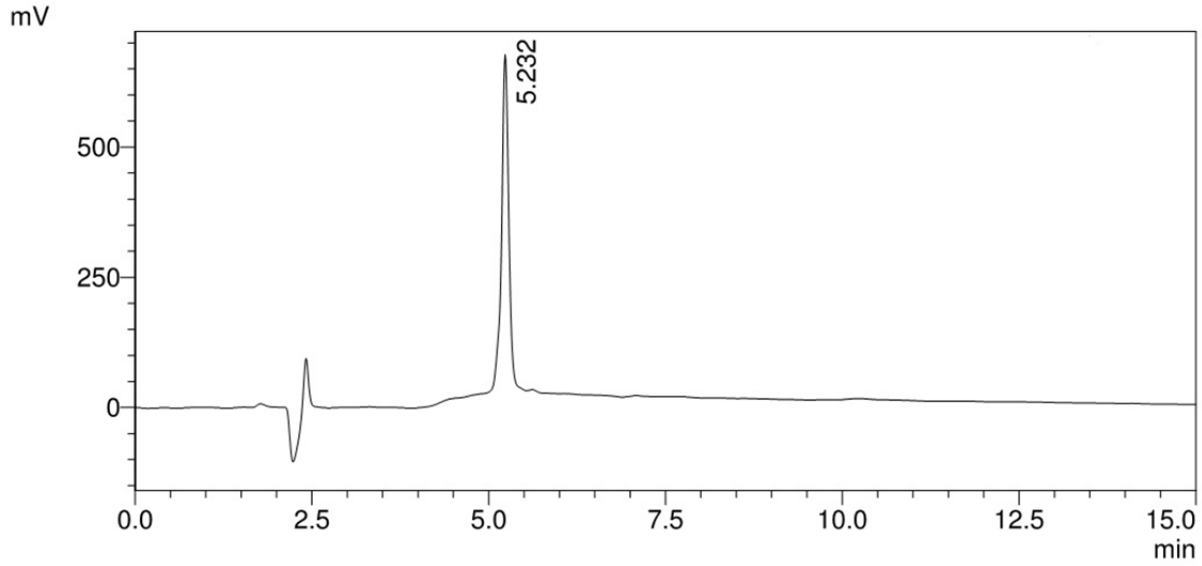

B)

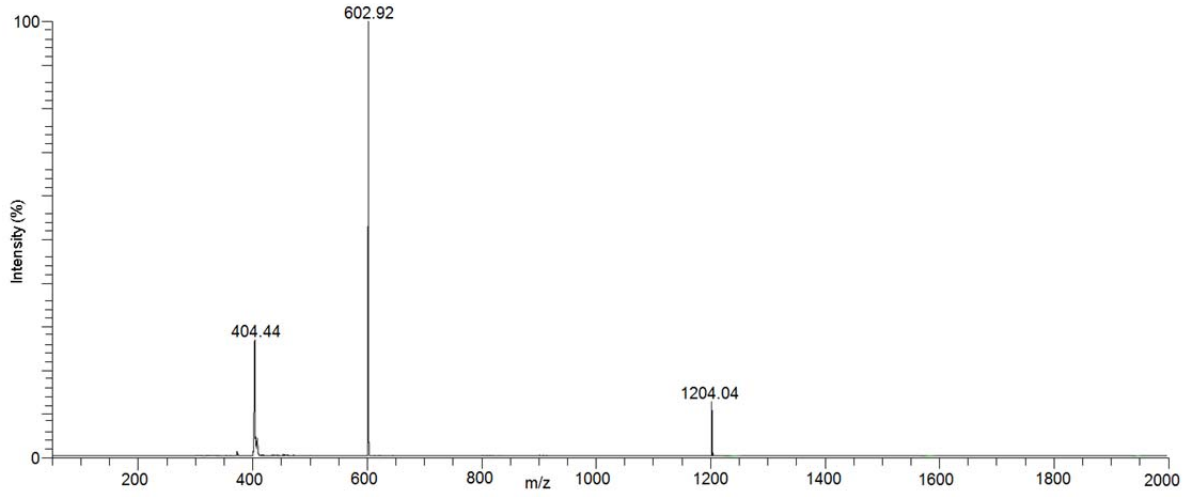

Fig. S7 (A) Analytical HPLC profile and **(B**) ESI-MS analysis of H3hK4Me3 peptide after prep-HPLC purification. The peptide elutes at 5.2 min. Calculated mass as $[M+H]^{+}$: 1204.44 Da, observed: 1204.04, 602.92 $[M+2H]^{2+}$, 404.44 $[M+3H]^{3+}$.

A)

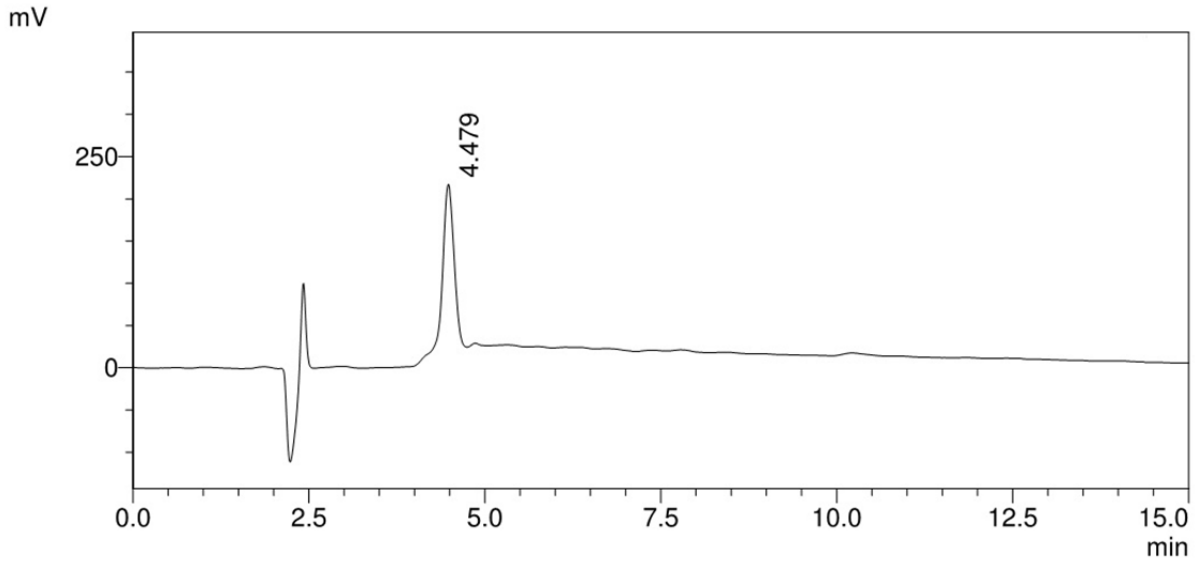

B)

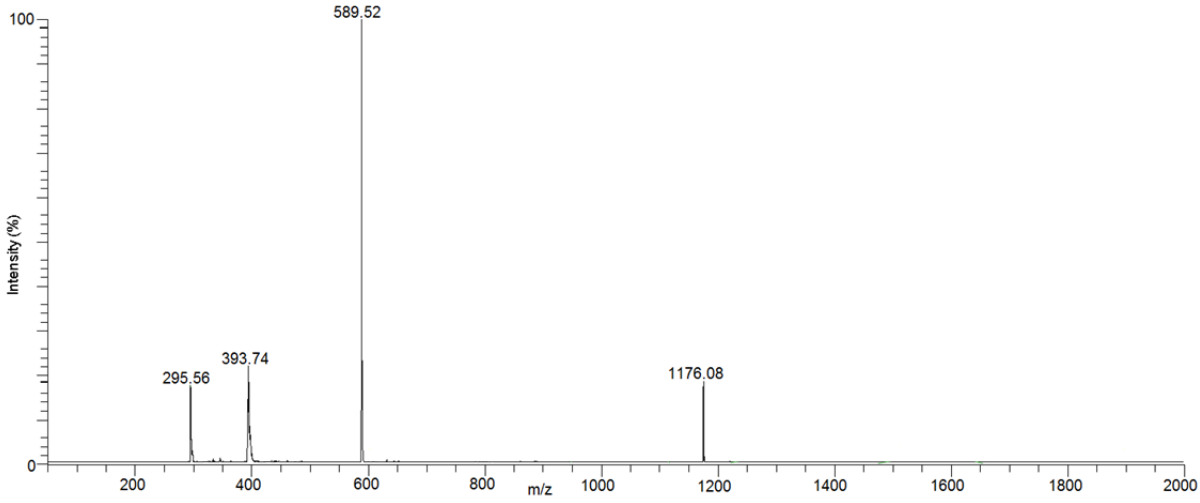

Fig. S8 (A) Analytical HPLC profile and **(B)** ESI-MS analysis of H3Orn4Me3 peptide after prep-HPLC purification. The peptide elutes at 4.5 min. Calculated mass as $[M+H]^{+}$: 1175.73 Da, observed: 1176.08, 589.52 $[M+2H]^{2+}$, 393.47 $[M+3H]^{3+}$, 295.56 $[M+4H]^{4+}$.

4. Isothermal titration calorimetry

Reader proteins used for ITC experiments were produced as described.[3] ITC analysis was done using a fully automated MicroCal Auto-iTC200 (GE Healthcare). Histone peptides and reader proteins were dissolved in the same buffer (used in size exclusion chromatography). Each ITC titration consisted of 19 injections of histone peptide (typically 400 μM) to reader protein (typically 27 μM). Experiments were repeated 3 to 5 times. Curve fitting was performed using Origin 6.0 (Microcal Inc., Northampton, MA) with a one-site mode.

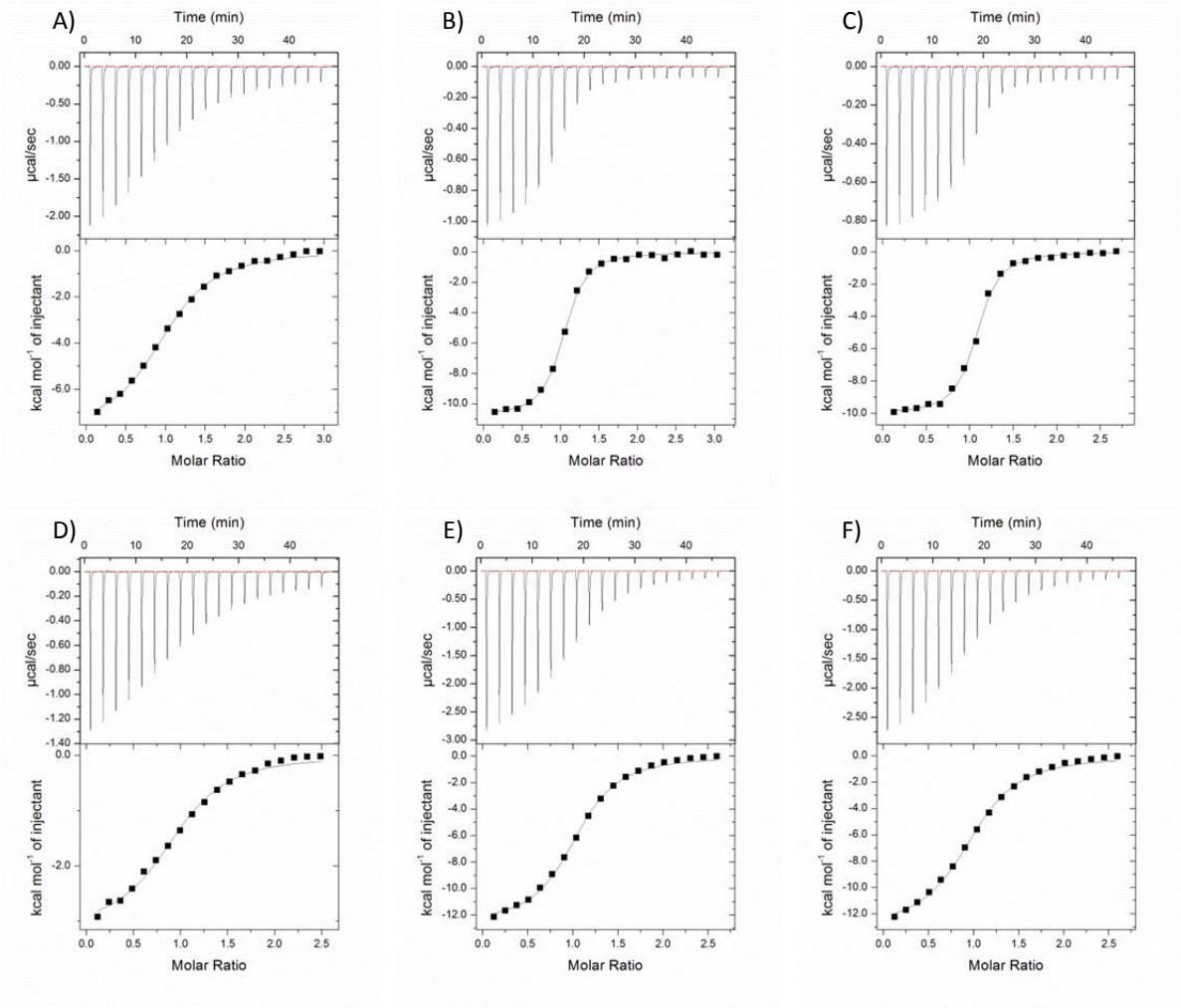

Fig. S9 Representative ITC data for binding of H3Orn4Me3, H3K4Me3, and H3hK4Me3 to KDM5A (top panel) and KDM4A (bottom panel). A) KDM5A–H3Orn4Me3; B) KDM5A–H3K4Me3; C) KDM5A–H3hK4Me3; D) KDM4A–H3Orn4Me3; E) KDM4A–H3K4Me3; F) KDM4A–H3hK4Me3.

5. Molecular dynamics simulations

Ten MD simulations were carried out for 10 ns each. A PDB structure for the model representing $TAF3_{PHD}$ (PDB: 2K17), $KDM4A_{TTD}$ (PDB: 2GFA), $KDM5A_{PHD3}$ (PDB: 2KGI), $BPTF_{PHD}$ (PDB: 2F6J), and $SGF29_{TTD}$ (PDB: 3ME9) reader proteins were used as a template for building the reader: OrnMe3 and hKMe3 systems. Initially, $KDM5A_{PHD3}$ was simulated for a longer timescale of 50 ns bound to OrnMe3 and hKMe3 to confirm equilibration could be reached for the reader:H3 systems. AMBER12[4] was used with the Amberff12SB force field to define protein partial charges. Hydrogen atom addition was performed with LEaP. Systems were solvated in a 10 Å truncated octahedral box of TIP3P[5] water and neutralised explicitly with either sodium or chloride counterions. Non-bonding parameters of Zn(II) previously established from studies of KDM4A(JMJD2A)[6,7] were employed. Atomic partial charges for OrnMe3 and hKMe3 ligands correspond to the Restrained Electrostatic Potential (RESP)[8] charges, shown in Tables S1-S2. Parameters for KMe3 taken from previous work.[2] The final systems were minimised for 1,000 cycles of steepest-descent minimization followed by 1,000 cycles of conjugate-gradient minimization to remove close van der Waals contacts using the *sander* program in AMBER12. Equilibration was achieved using PMEMD to heat the systems to 310 K followed by independent MD simulations performed with a periodic boundary condition at a constant pressure of 1 atm with isotropic molecule-based scaling at a time step of 2.0 fs. All simulations used a dielectric constant of 1.0, Particle Mesh Ewald summation[9] to calculate long-range electrostatic interactions and bond-length constraints applied to all bonds to H atoms. No restraints were used on the protein or ligands. Trajectories were saved at 20-ps intervals and visualised using VMD.[10] Electrostatic energies between the terminal modified KMe3 side chain N^{ε} atom and the π-system of surrounding aromatic cages were calculated with the NAMDEnergy Plugin 1.[10] The π-system was defined for tryptophan, tyrosine, and phenylalanine residues as the ring (non-H) atoms. Energy values were measured every 20 ps and averaged over 10 ns.

Table S1 Cartesian coordinates and charges calculated using the RESP method HF/6-31G* of modified OrnMe3 residues used in MD simulations.

OrnMe3 Atom	X	Y	Z	RESP Charge
N	-2.484	1.459	0.074	-0.996696
C	-2.467	0.129	-0.495	0.394184
C	-1.242	-0.652	0.013	-0.349661
C	0.068	0.042	-0.378	0.305879
C	1.251	-0.669	0.272	-0.196384
C	-3.720	-0.680	-0.184	0.393279
O	-4.532	-0.330	0.605	-0.461126
H	-2.906	1.429	0.984	0.383628
H	-3.063	2.068	-0.473	0.383628
H	-2.394	0.211	-1.577	0.005175
H	-1.260	-1.667	-0.375	0.094726
H	-1.310	-0.726	1.096	0.094726
H	0.163	0.030	-1.459	-0.019932
H	0.000	1.072	-0.061	-0.019932
H	1.346	-1.679	-0.104	0.124069
H	1.116	-0.722	1.344	0.124069
H	-3.824	-1.630	-0.718	0.013141
N	2.610	-0.024	0.065	0.178239
C	2.946	0.077	-1.387	-0.378967
H	2.863	-0.901	-1.837	0.187321
H	2.269	0.764	-1.868	0.187321
H	3.958	0.440	-1.485	0.187321
C	3.633	-0.886	0.734	-0.378967
H	4.608	-0.439	0.611	0.187321
H	3.397	-0.964	1.785	0.187321
H	3.621	-1.866	0.282	0.187321
C	2.659	1.338	0.683	-0.378967
H	2.387	1.262	1.725	0.187321
H	3.664	1.721	0.594	0.187321
H	1.976	1.995	0.171	0.187321

Table S2 Cartesian coordinates and charges calculated using the RESP method HF/6-31G* of modified hMe3 residues used in MD simulations.

hMe3 Atom	X	Y	Z	RESP Charge
N	3.844	1.498	-0.189	-0.993558
C	3.798	0.199	0.448	0.419383
C	2.550	-0.580	0.001	-0.233717
C	1.250	0.113	0.411	0.124829
C	0.009	-0.596	-0.138	-0.048834
C	-1.286	0.134	0.250	0.056981
C	5.031	-0.652	0.181	0.368966
O	5.874	-0.353	-0.599	-0.469423
H	4.176	1.397	-1.130	0.374567
H	4.511	2.088	0.271	0.374567
H	3.739	0.344	1.525	-0.002661
H	2.578	-1.586	0.416	0.058341
H	2.583	-0.688	-1.081	0.058341
H	1.191	0.154	1.496	-0.010380
H	1.277	1.136	0.058	-0.010380
H	-0.027	-1.619	0.230	0.028014
H	0.077	-0.655	-1.221	0.028014
H	-1.355	0.178	1.331	0.024116
H	-1.233	1.153	-0.116	0.024116
H	5.095	-1.588	0.745	0.008756
C	-2.490	-0.593	-0.341	-0.134217
H	-2.542	-1.604	0.038	0.111937
H	-2.407	-0.643	-1.418	0.111937
N	-3.853	0.019	-0.065	0.194742
C	-4.883	-0.844	-0.722	-0.376156
H	-4.826	-1.840	-0.309	0.184893
H	-5.862	-0.428	-0.540	0.184893
H	-4.691	-0.877	-1.784	0.184893
C	-3.952	1.397	-0.636	-0.376156
H	-3.272	2.054	-0.120	0.184893
H	-3.706	1.362	-1.686	0.184893
H	-4.963	1.753	-0.509	0.184893
C	-4.137	0.067	1.402	-0.376156
H	-5.149	0.412	1.548	0.184893
H	-4.025	-0.924	1.815	0.184893
H	-3.453	0.747	1.881	0.184893

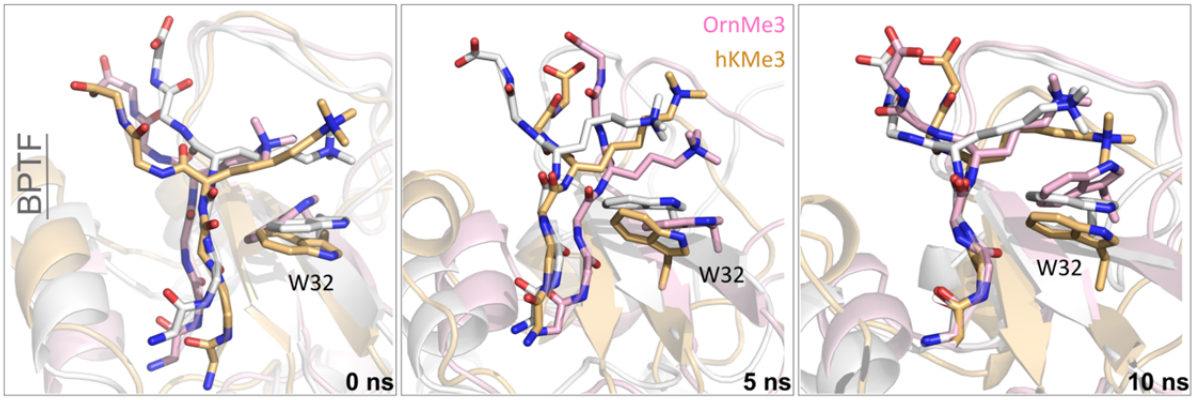

Fig. S10 Snapshots of reader BPTF complexed with histone 3 chain backbone (liqorice) containing OrnMe3 (pink), hKMe3 (orange), and KMe3 (white) active site at times 0 ns, 5ns, and 10 ns. (PDB 2F6J).

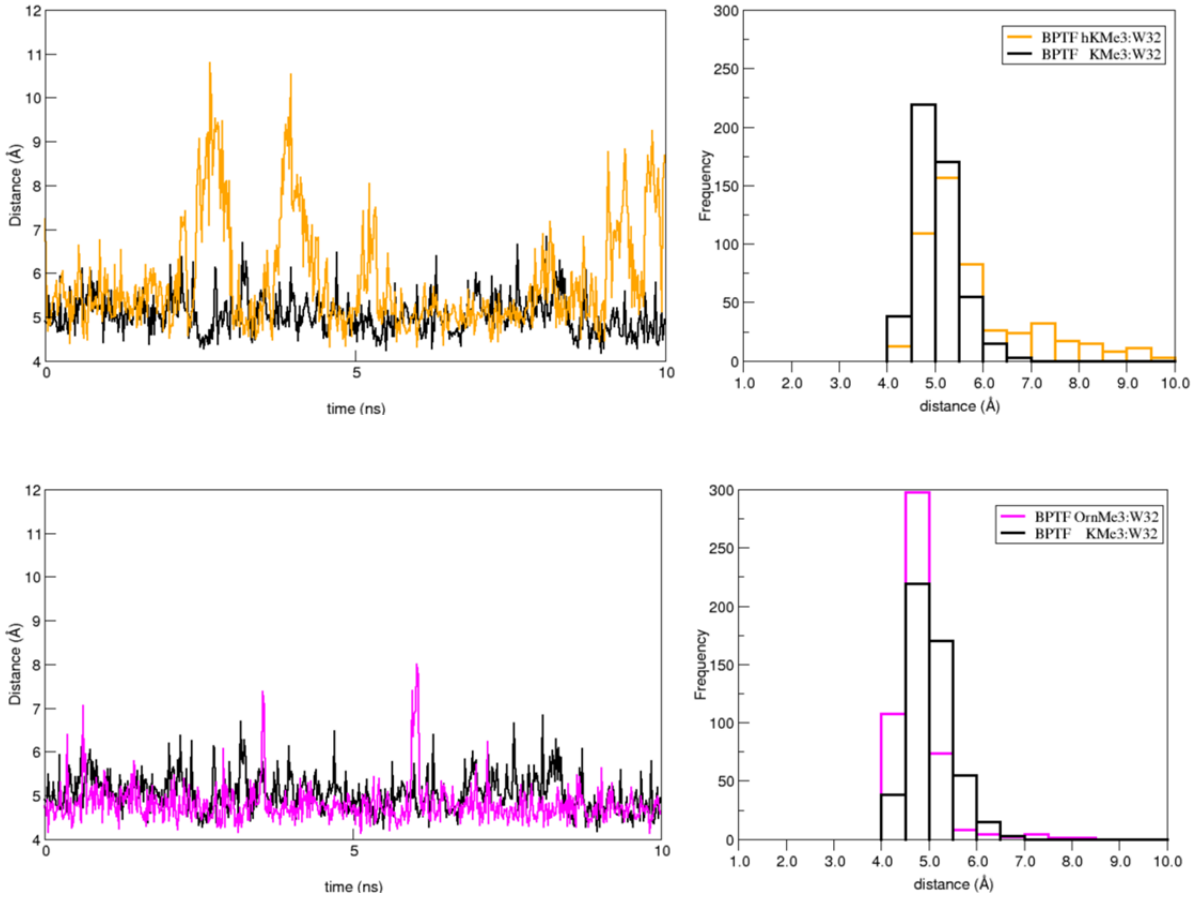

Fig. S11 Distance vs. time plots of $^{\varepsilon}N^{+}$ atom of hKMe3, OrnMe3, and KMe3 to W32 side chain center of mass over 10 ns.

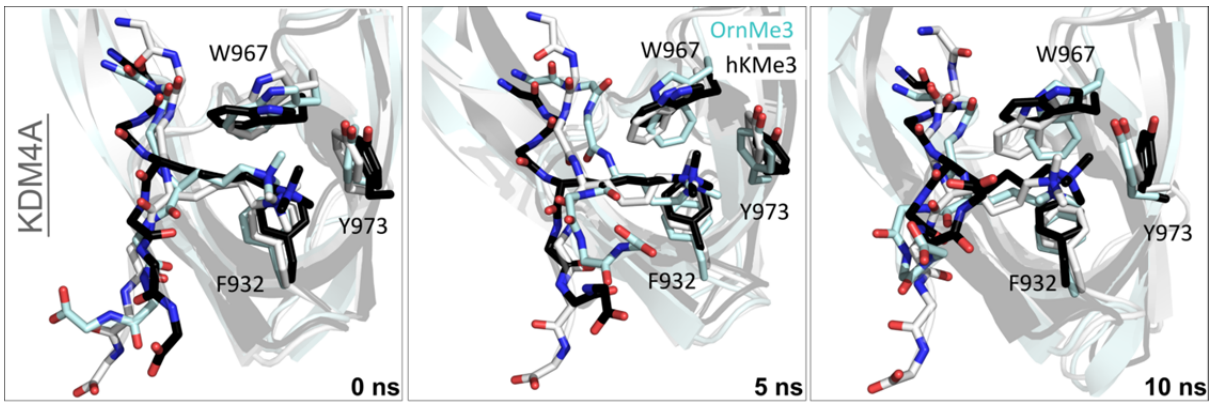

Fig. S12 Snapshots of reader KDM4A complexed with histone 3 chain backbone (liqorice) containing OrnMe3 (blue), hKMe3 (black), and KMe3 (white) active site at times 0 ns, 5ns, and 10 ns. (PDB 2GFA).

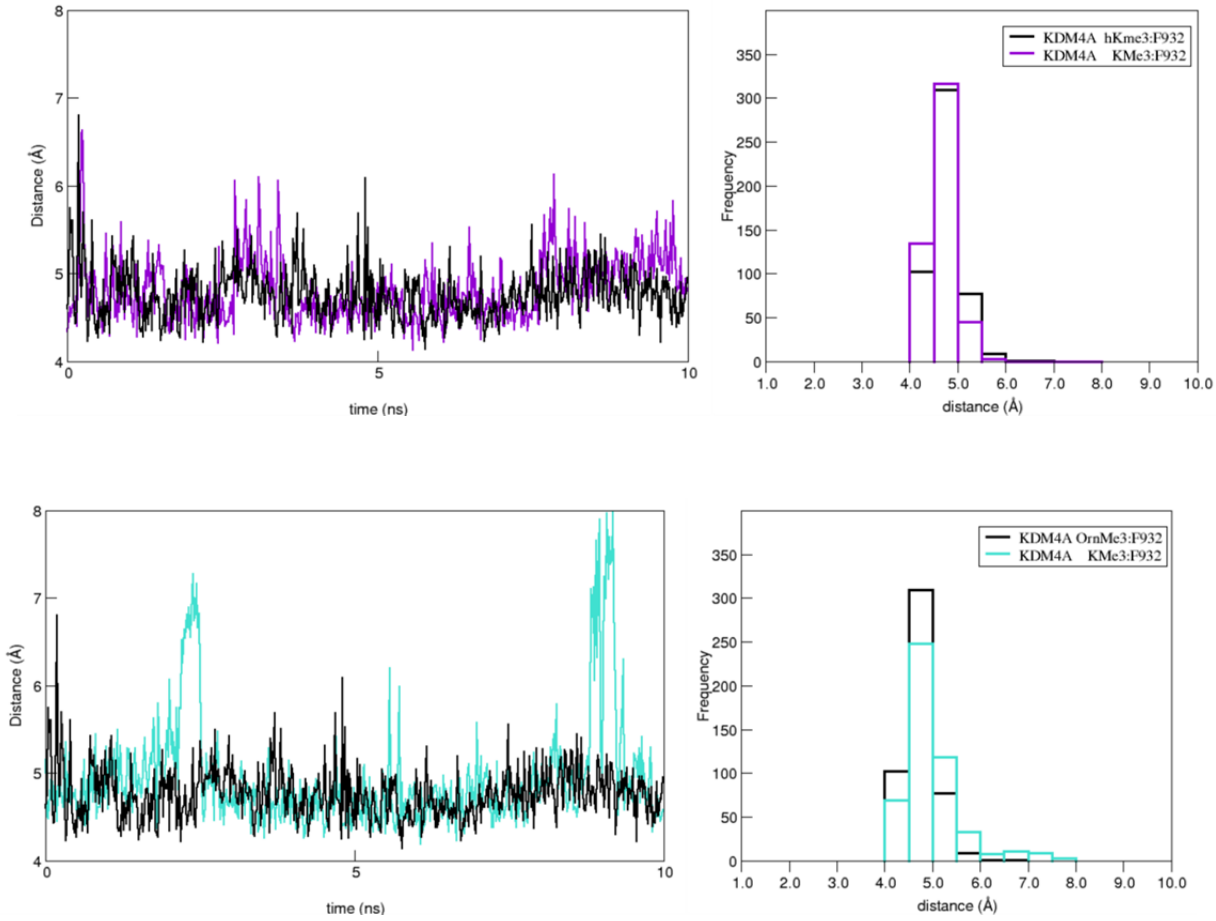

Fig. S13 Distance vs. time plots of $^{\varepsilon}N^{+}$ atom of hKME3, OrnMe3, and KMe3 to F932 side chain center of mass over 10 ns.

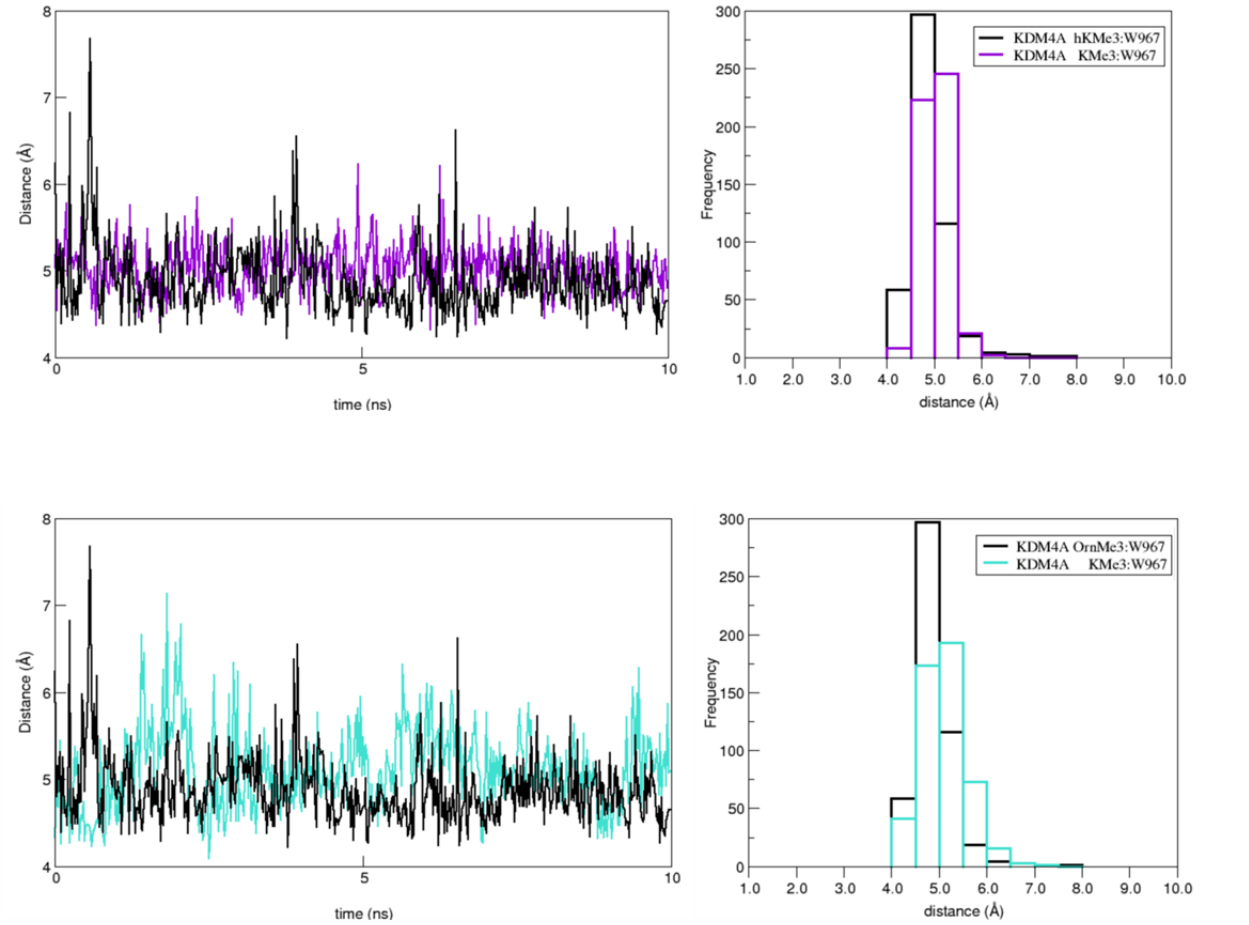

Fig. S14 Distance vs. time plots of $^{\varepsilon}N^{+}$ atom of hKMe3, OrnMe3, and KMe3 to W967 side chain center of mass over 10 ns.

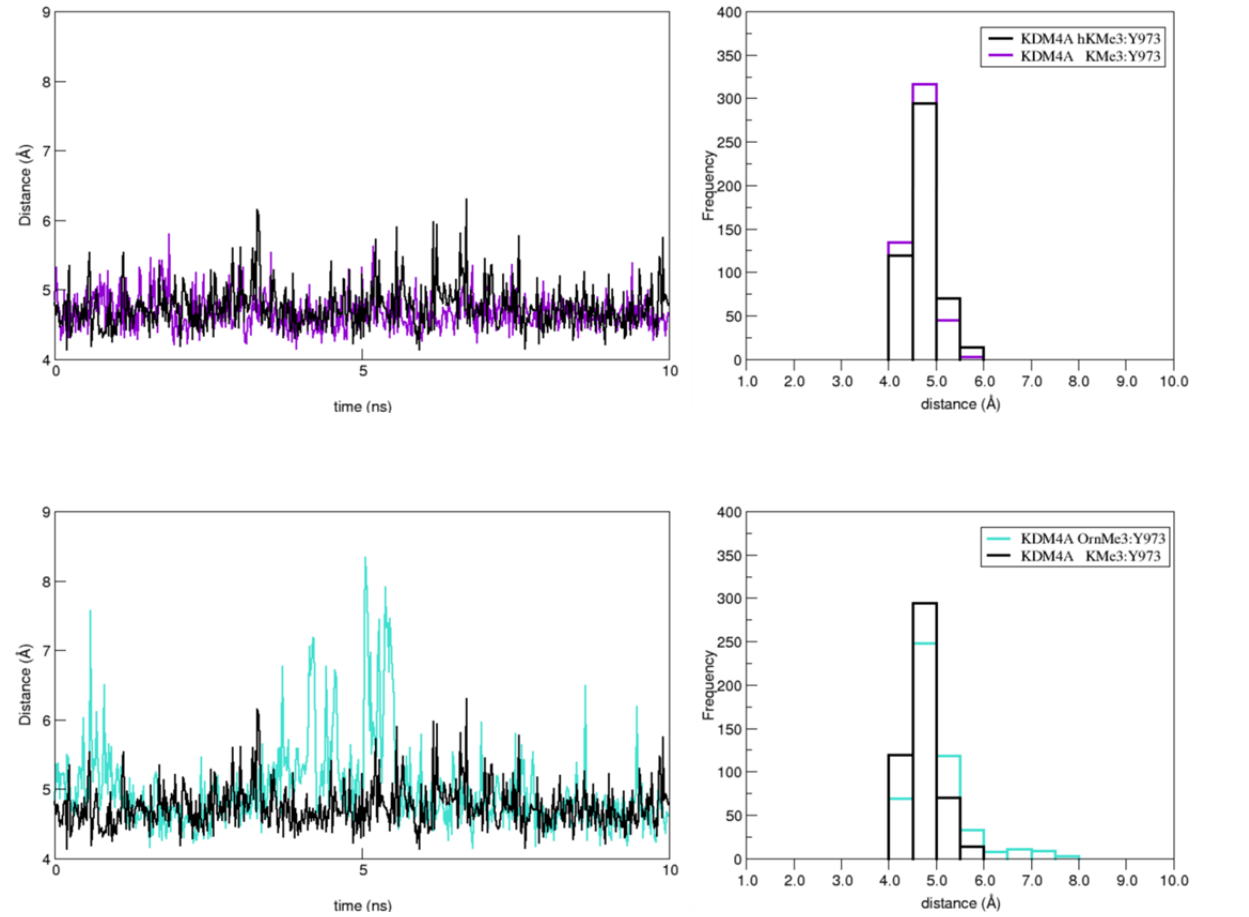

Fig. S15 Distance vs. time plots of $^{\varepsilon}N^{+}$ atom of hKMe3, OrnMe3, and KMe3 to Y973 side chain center of mass over 10 ns.

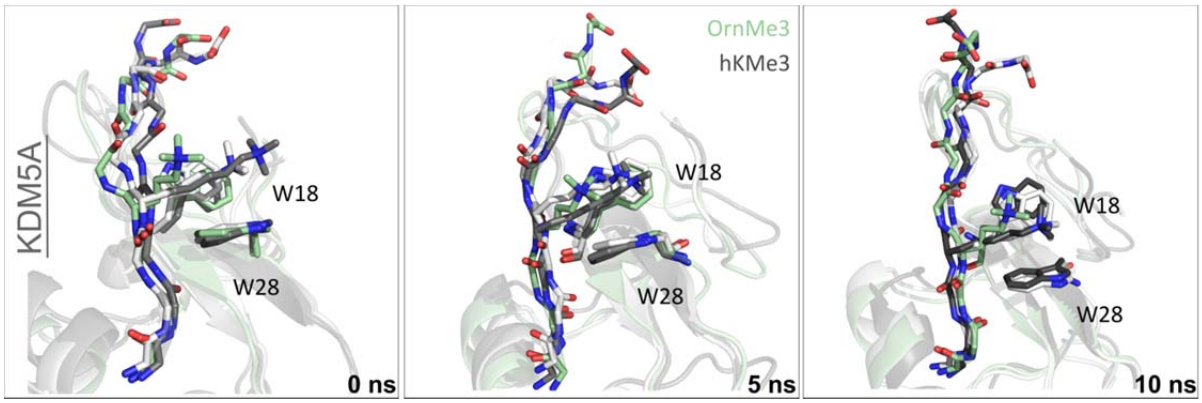

Fig. S16 Snapshots of reader KDM5A complexed with histone 3 chain backbone (liqorice) containing OrnMe3 (light green), hKMe3 (dark green), and KMe3 (white) active site at times 0 ns, 5ns, and 10 ns. (PDB 2KGI).

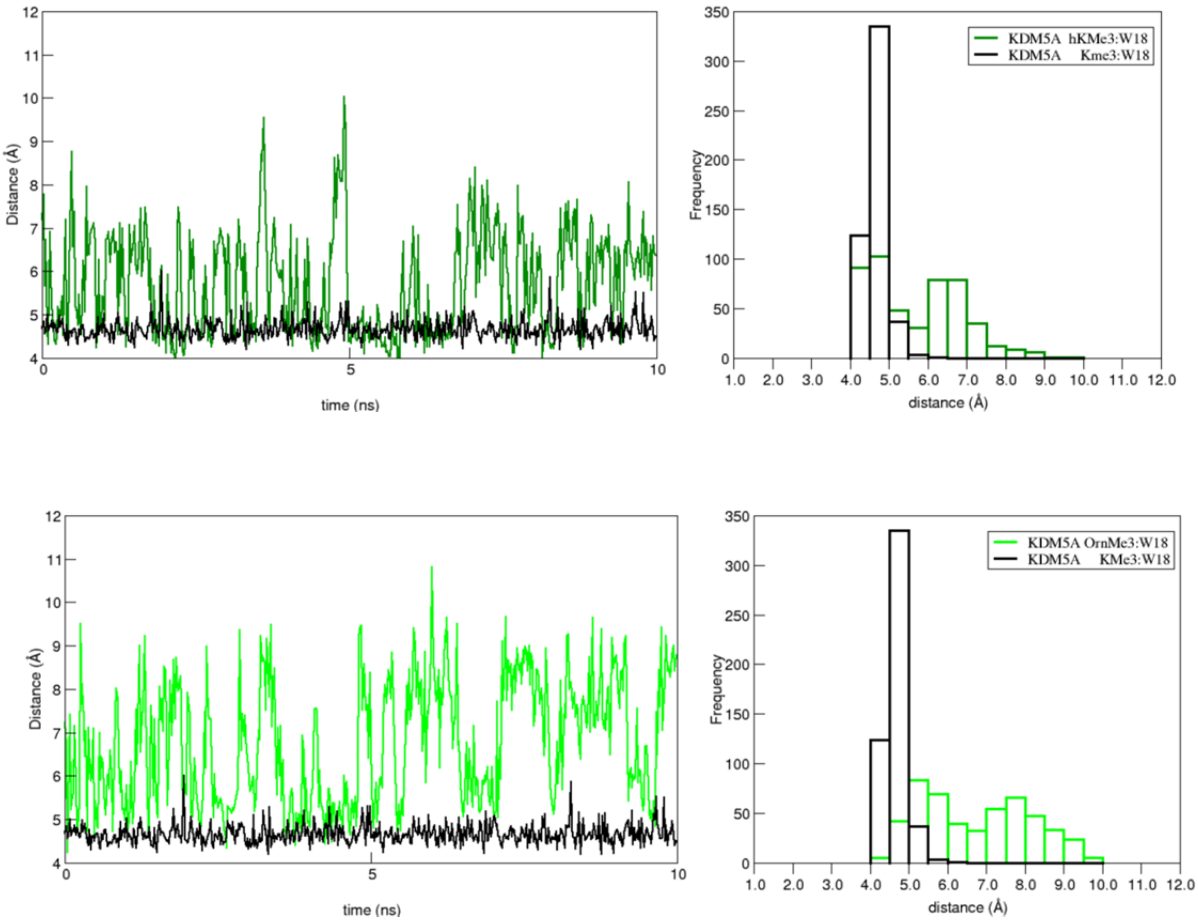

Fig. S17 Distance vs. time plots of $^{\varepsilon}N^{+}$ atom of hKME3, OrnMe3, and KMe3 to W18 side chain center of mass over 10 ns.

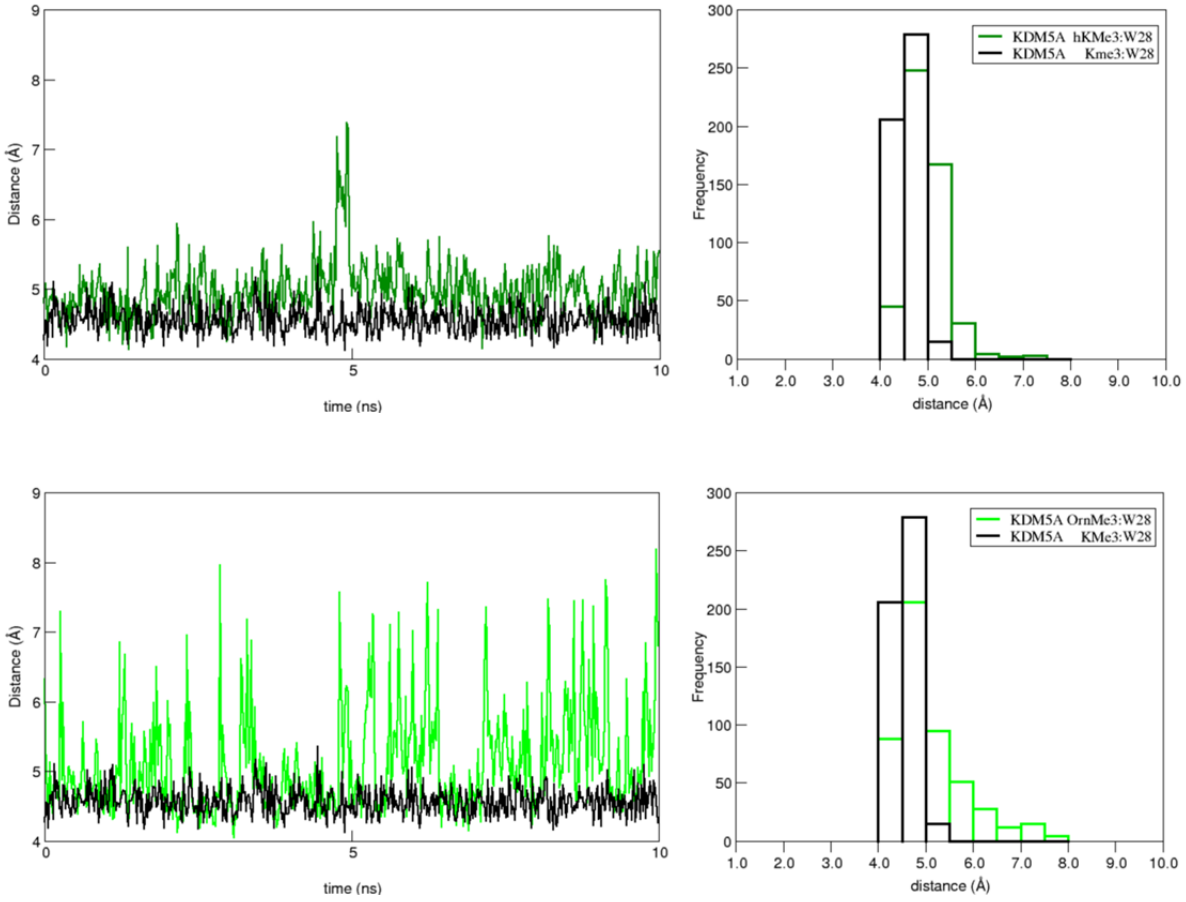

Fig. S18 Distance vs. time plots of $^{\varepsilon}N^{+}$ atom of hKMe3, OrnMe3, and KMe3 to W28 side chain center of mass over 10 ns.

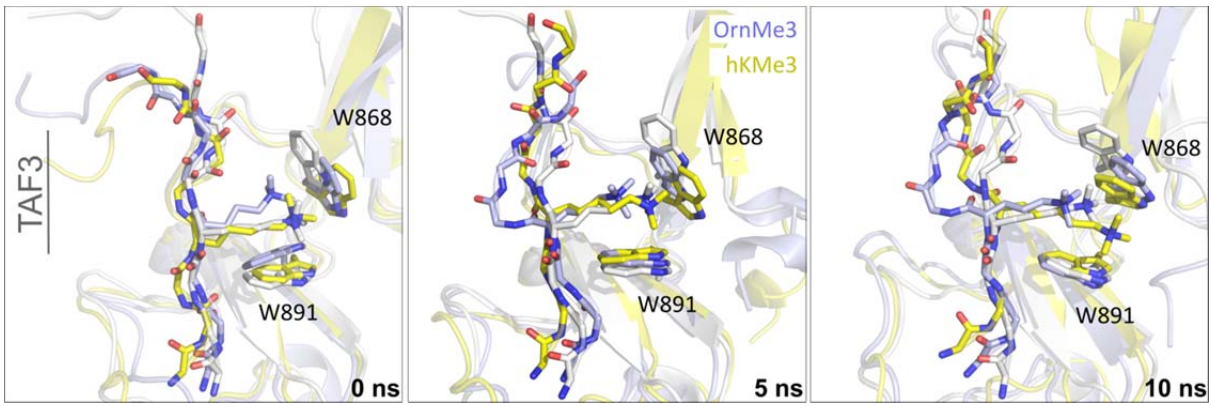

Fig. S19 Snapshots of reader TAF3 complexed with histone 3 chain backbone (liqorice) containing OrnMe3 (blue), hKMe3 (yellow), and KMe3 (white) active site at times 0 ns, 5ns, and 10 ns. (PDB 2K17).

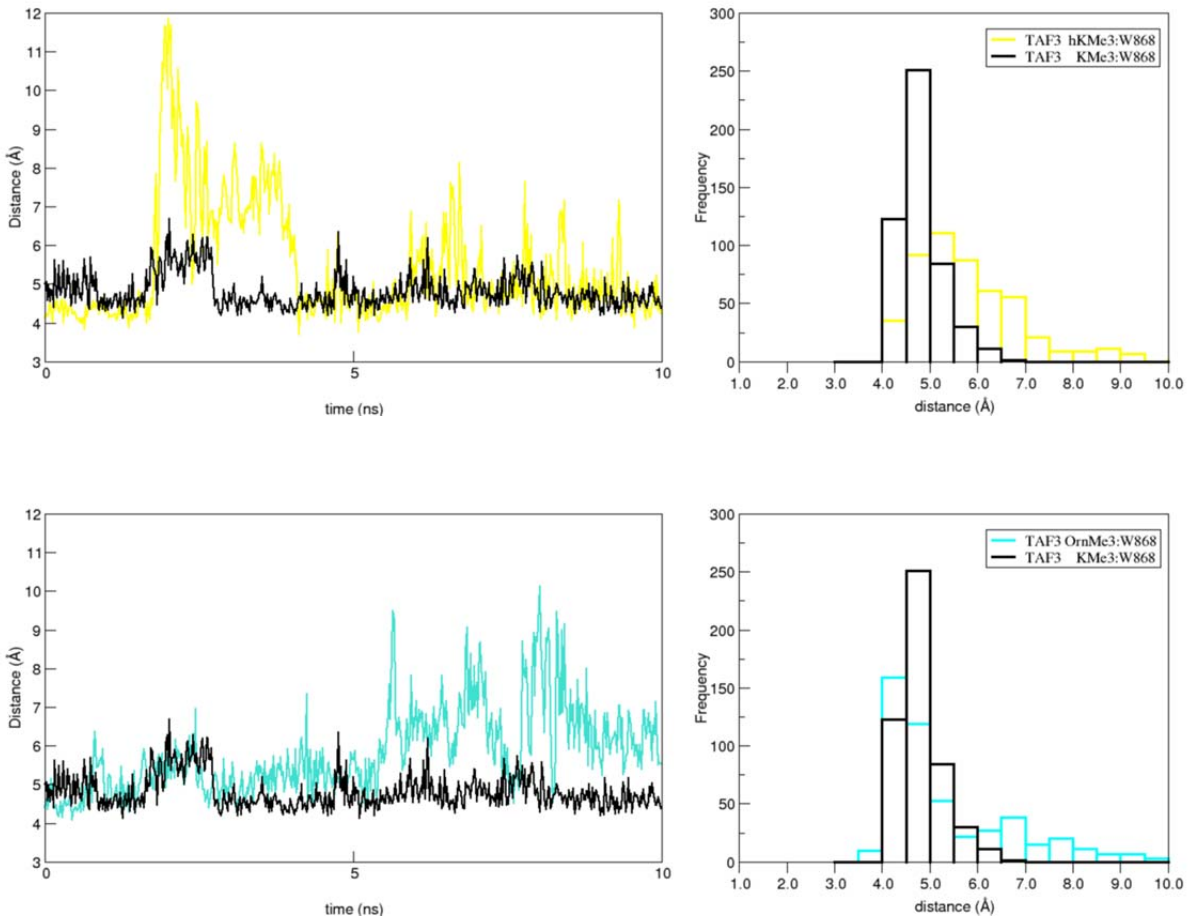

Fig. S20 Distance vs. time plots of $^{\varepsilon}N^{+}$ atom of hKMe3, OrnMe3, and KMe3 to W868 side chain center of mass over 10 ns.

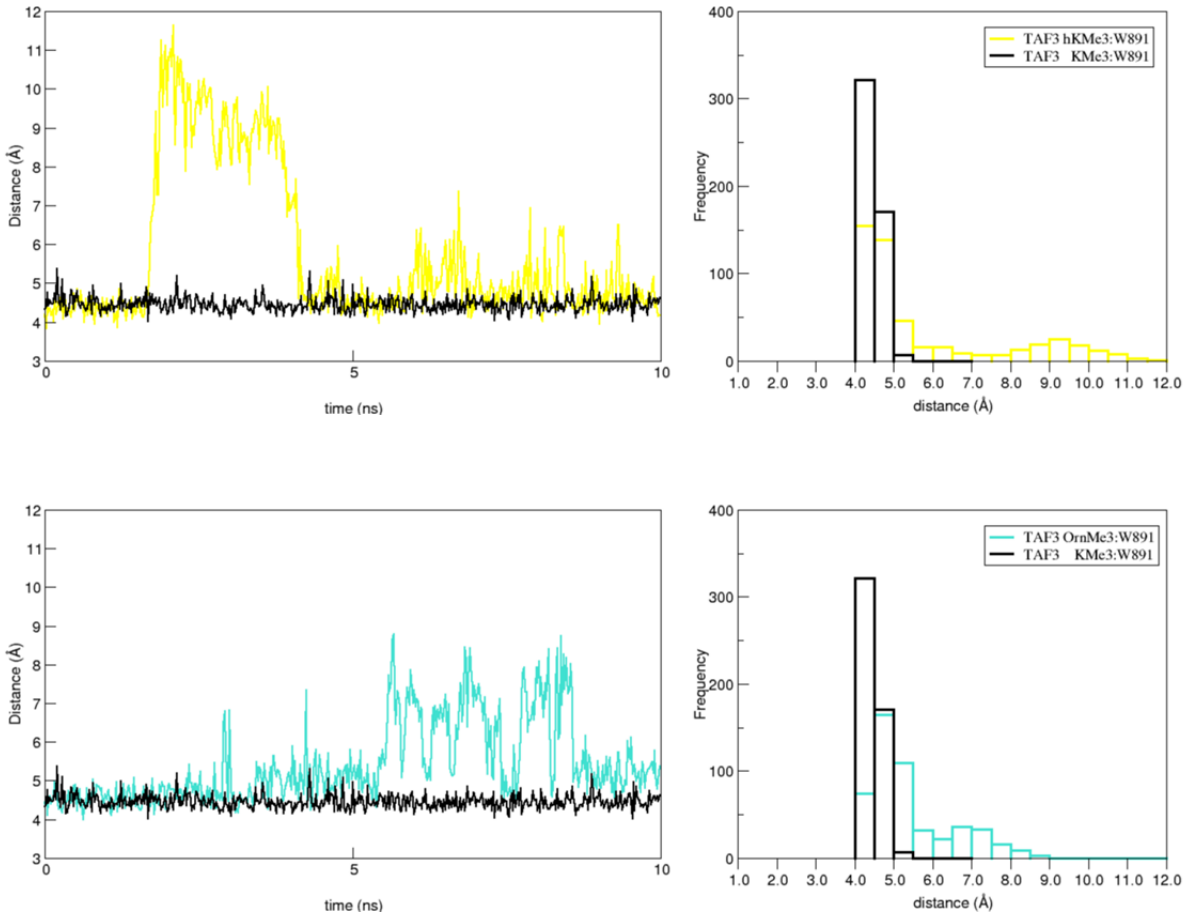

Fig. S21 Distance vs. time plots of $^{\varepsilon}N^{+}$ atom of hKMe3, OrnMe3, and KMe3 to W891 side chain center of mass over 10 ns.

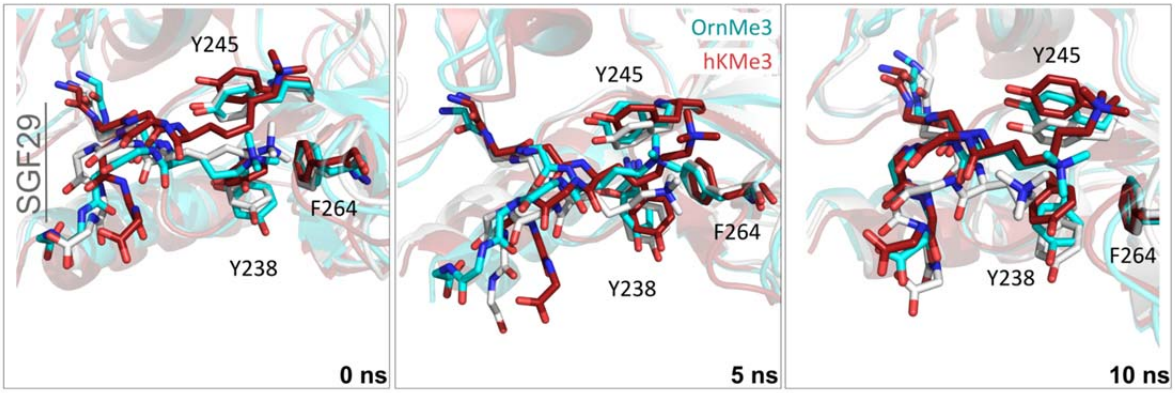

Fig. S22 Snapshots of reader SGF29 complexed with histone 3 chain backbone (liqorice) containing OrnMe3 (blue), hKMe3 (red), and KMe3 (white) active site at times 0 ns, 5ns, and 10 ns. (PDB 3ME9).

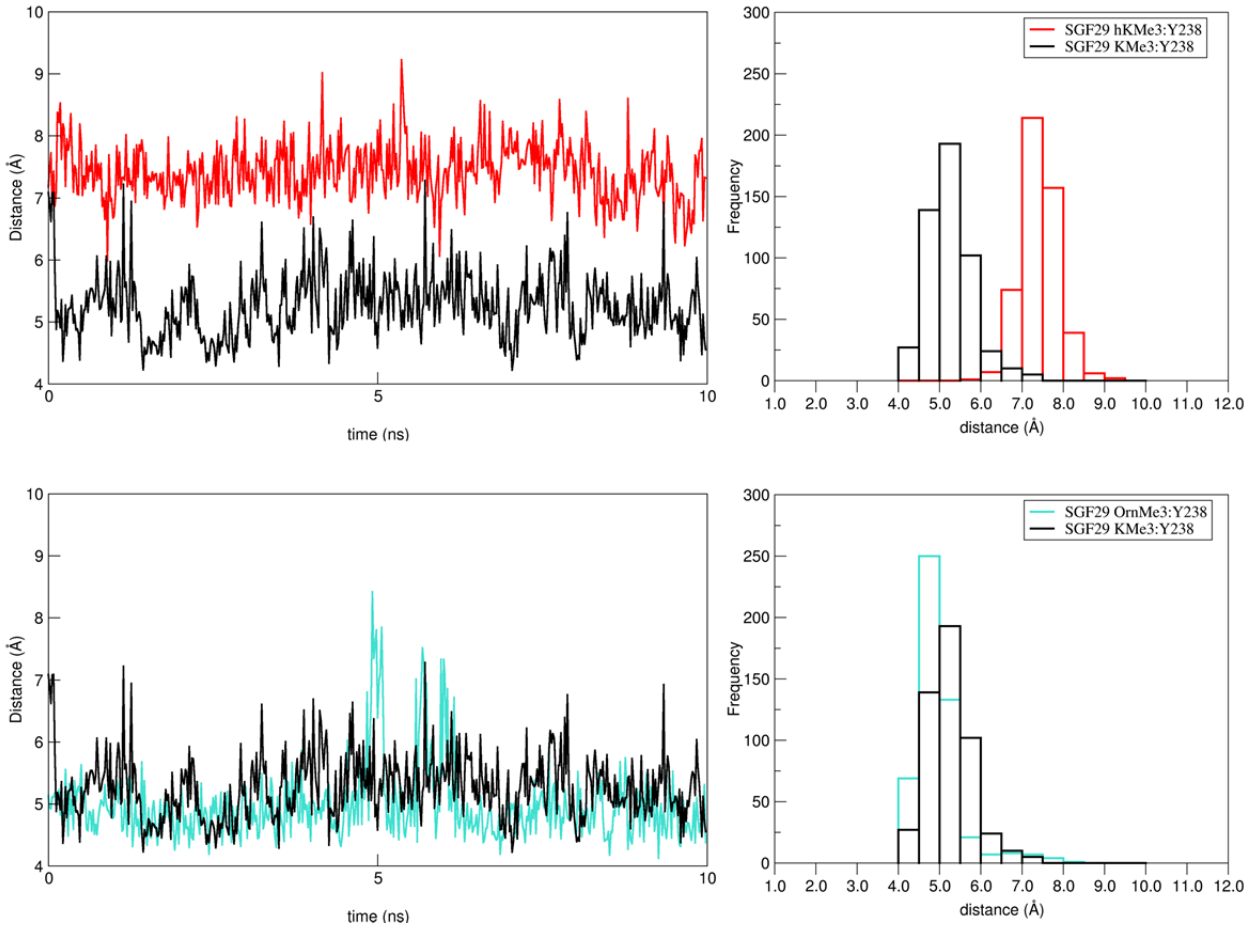

Fig. S23 Distance vs. time plots of $^{\varepsilon}N^{+}$ atom of hKMe3, OrnMe3, and KMe3 to Y238 side chain center of mass over 10 ns.

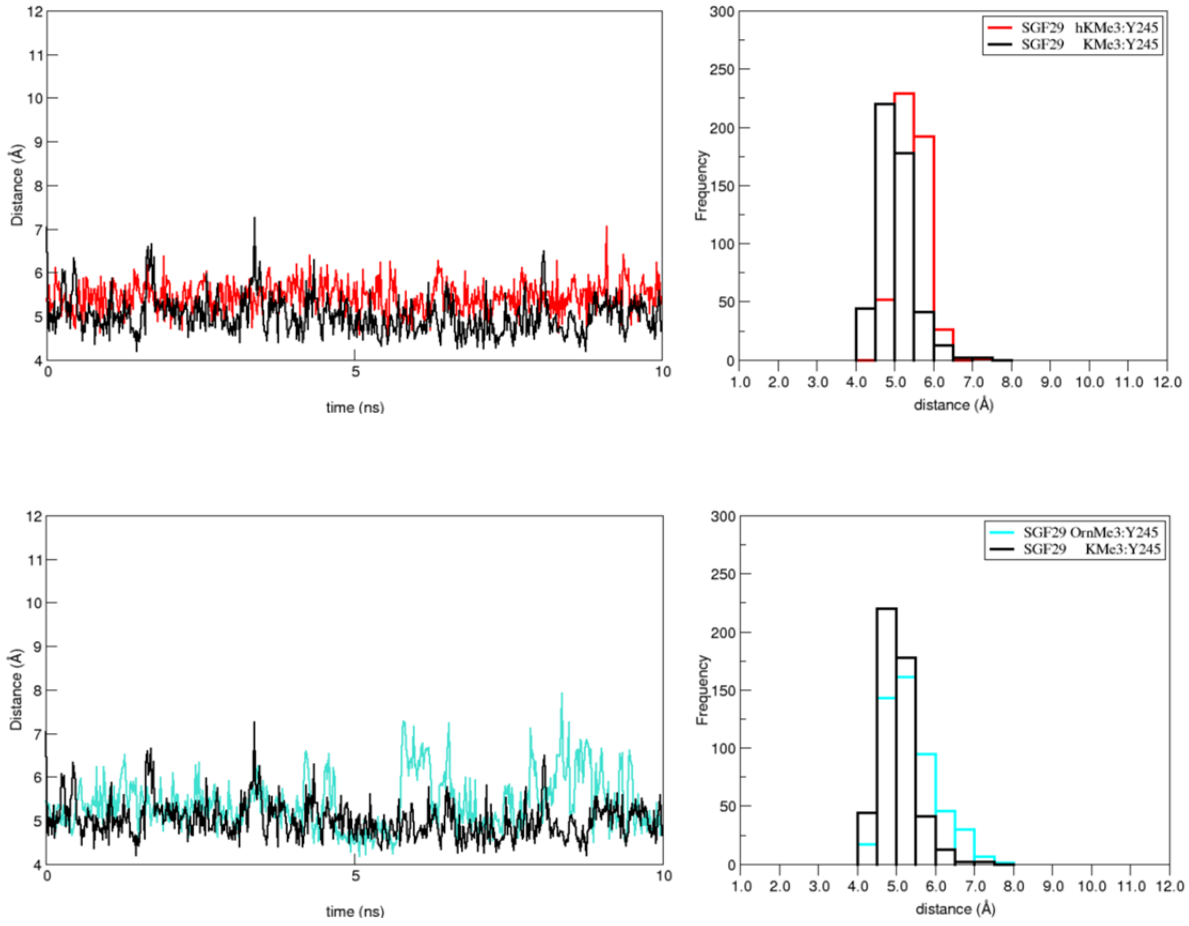

Fig. S24 Distance vs. time plots of $^{\varepsilon}N^{+}$ atom of hKMe3, OrnMe3, and KMe3 to Y245 side chain center of mass over 10 ns.

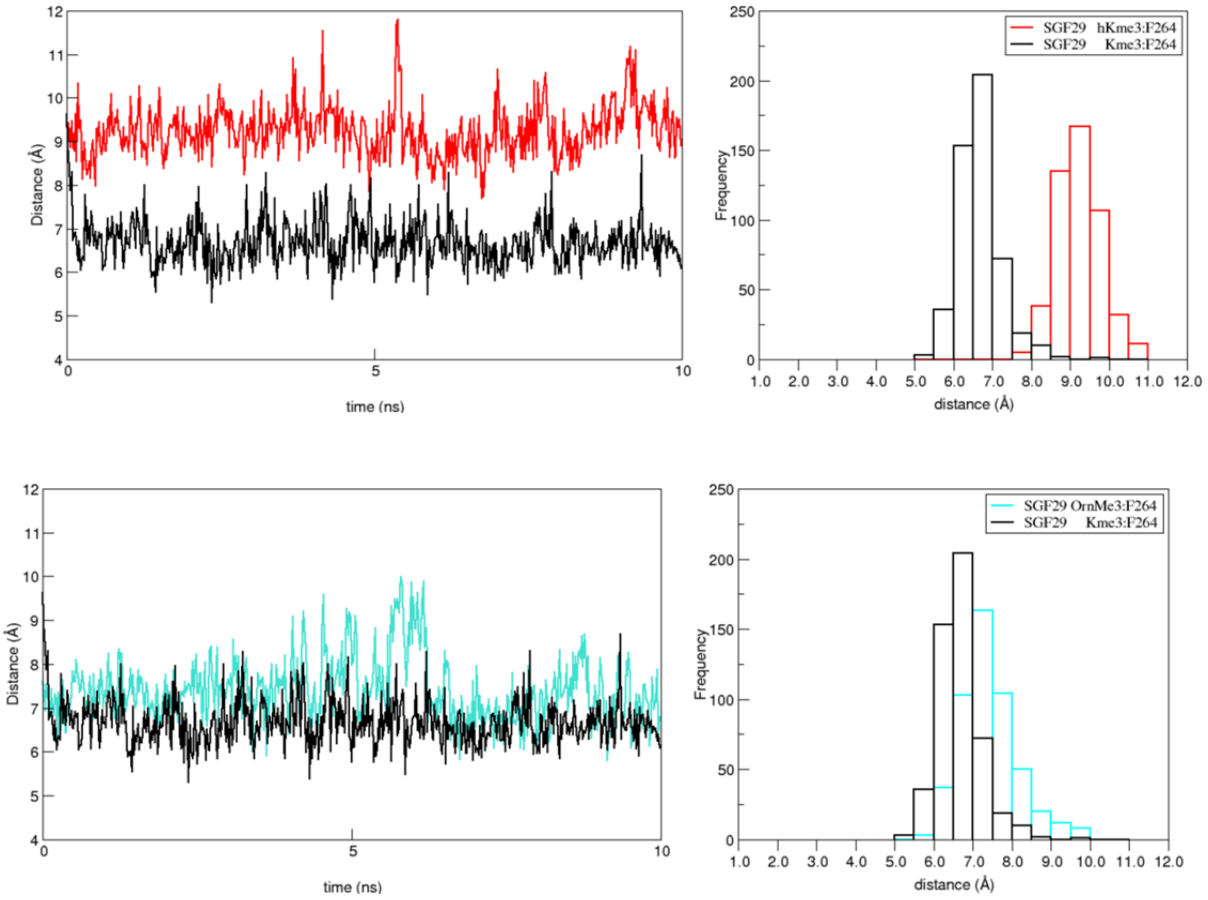

Fig. S25 Distance vs. time plots of $^{\varepsilon}N^{+}$ atom of hKME3, OrnMe3, and KME3 to F264 side chain center of mass over 10 ns.

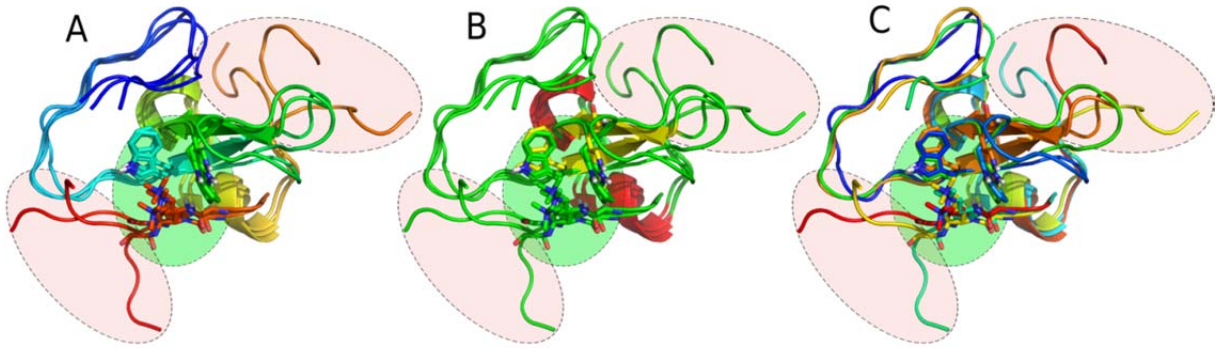

Fig. S26 Overlaid structures of KDM5A bound to H3 containing OrnMe3 at times 0 ns, 25 ns, and 50 ns and visualized in three different representations. RGB spectrum represents different properties. A) is coloured by sequence for each structure, where red is the C-terminus of H3 and blue is the N-terminus of KDM5A. B) is coloured by secondary structure where red, yellow, and green represent β-sheet, α-helix, and random coil, respectively. C) is coloured by simulation time where the red, yellow, and blue structures show the protein at time 0 ns, 25 ns, and 50 ns, respectively. Red circles highlight highly flexible random coil regions of the protein and green circles highlight the rigid core containing the aromatic TRP2 cage and OrnMe3 ligand.

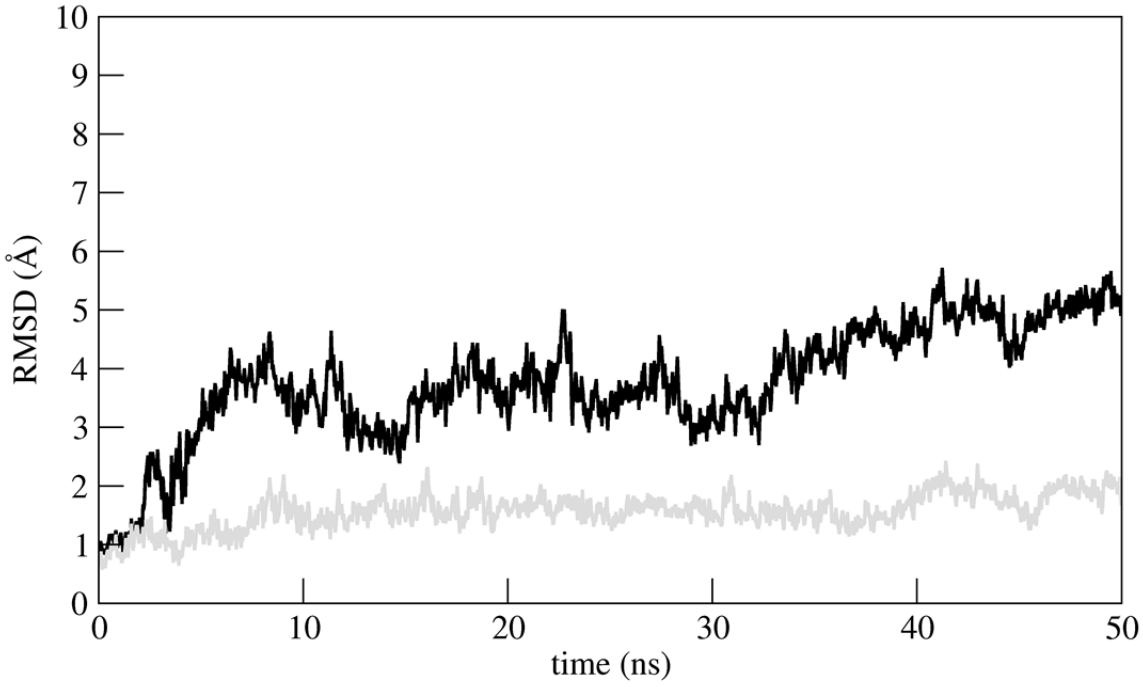

Fig. S27 RMSD plot of KDM5A complexed with OrnKme3 Cα atoms over 50 ns (grey, 1.56 ± 0.30), and including random coil KDM5A and H3 terminal residues 47-52, 58-61, and 23-25 (black, 3.76 ± 0.98).

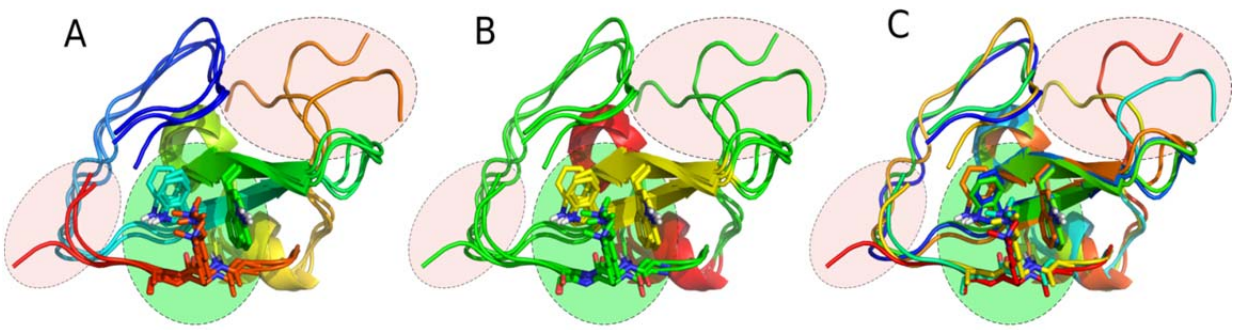

Fig. S28 Overlaid structures of KDM5A bound to H3 containing hKMe3 at times 0 ns, 25 ns, and 50 ns and visualized in three different representations. RGB spectrum represents different properties. A) is coloured by sequence for each structure, where red is the C-terminus of H3 and blue is the N-terminus of KDM5A. B) is coloured by secondary structure where red, yellow, and green represent β-sheet, α-helix, and random coil, respectively. C) is coloured by simulation time where the red, yellow, and blue structures show the protein at time 0 ns, 25 ns, and 50 ns, respectively. Red circles highlight highly flexible random coil regions of the protein and green circles highlight the rigid core containing the aromatic TRP2 cage and hKMe3 ligand.

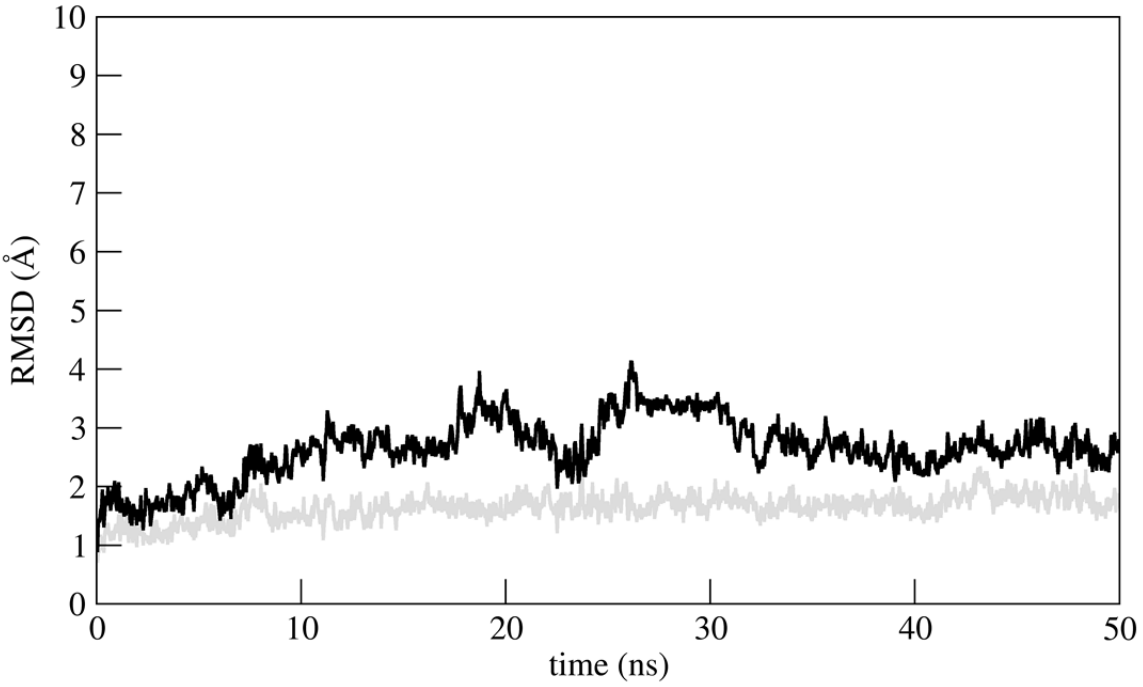

Fig. S29 RMSD plot of KDM5A complexed with hKMe3 Cα atoms over 50 ns (grey, 1.64 ± 0.23), and including random coil KDM5A and H3 terminal residues 47-52, 58-61, and 23-25 (black, 2.65 ± 0.51).

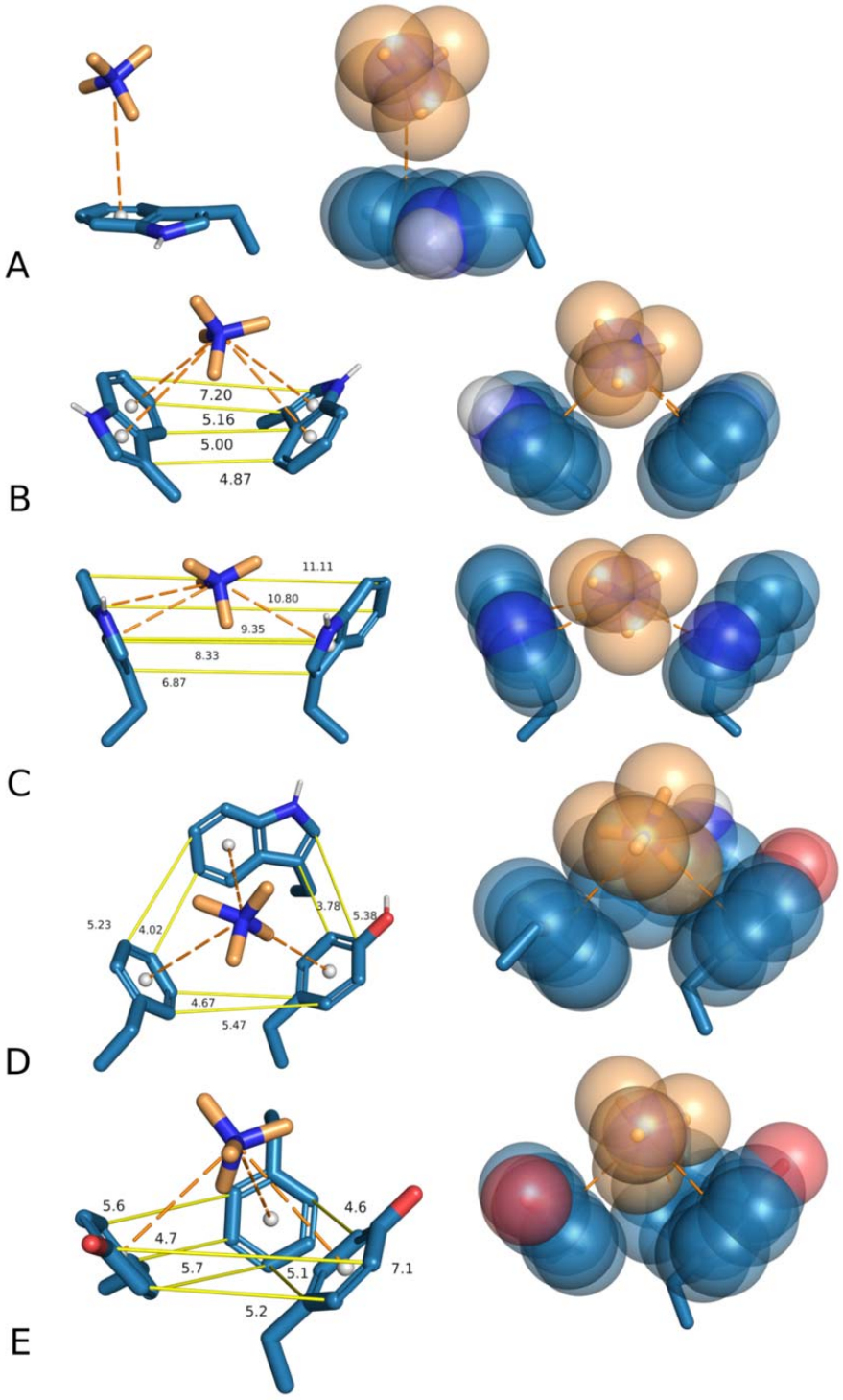

Fig. S30 Schematic and van Der Waals visualization highlight the different cation-π interactions with aromatic cage of readers A) BPTF, B) KDM5A, C) TAF3, D) KDM4A, and E) SGF29. Distances in Å. Structures taken from crystal structures (see computational methodology).

Table S3 Average root mean square deviation (RMSD) and error of C^{α} atoms of reader proteins.

	RMSD (Å)		
		Reader	**H3**
BPTF	hKMe3	3.32 ± 0.93	0.71 ± 0.26
	KMe3	5.85 ± 2.49	0.47 ± 0.20
	OrnMe3	7.10 ± 1.97	0.79 ± 0.35
KDM5A	hKMe3	1.77 ± 0.42	1.58 ± 0.44
	KMe3	0.25 ± 0.58	1.16 ± 0.34
	OrnMe3	2.77 ± 1.17	1.23 ± 0.43
KDM4A	hKMe3	2.20 ± 0.76	1.96 ± 0.18
	KMe3	2.08 ± 0.64	1.17 ± 0.27
	OrnMe3	3.68 ± 0.89	1.98 ± 0.47
SGF29	hKMe3	1.17 ± 0.14	0.57 ± 0.12
	KMe3	1.28 ± 0.20	1.03 ± 0.45
	OrnMe3	1.21 ± 0.14	1.61 ± 0.86
TAF3	hKMe3	3.15 ± 0.64	4.70 ± 1.35
	KMe3	3.25 ± 0.82	3.24 ± 1.20
	OrnMe3	3.87 ± 0.64	3.14 ± 0.84

Table S4 Average calculated Coulombic electrostatic energy (ΔE_{ele}) between the terminal $^{\varepsilon}N^{+}$ atom of the histone peptides H3Orn4Me3, H3K4Me3, and H3hK4Me3 to the π-system of reader protein aromatic cage residues over 10 ns.

		ΔE_{ele} (kcal mol^{-1})		
		hKMe3	**KMe3**	**OrnMe3**
BPTF	W32	-7.9 ± 2.7	-12.0 ± 1.6	-9.5 ± 1.2
KDM5A	W18	-7.9 ± 3.1	-13.0 ± 1.0	-5.1 ± 2.6
	W28	-9.9 ± 1.3	-13.2 ± 0.9	-8.8 ± 1.8
KDM4A	W967	-9.6 ± 0.8	-12.2 ± 1.5	-8.8 ± 1.2
	Y973	-9.8 ± 0.9	-11.9 ± 1.4	-8.8 ± 1.2
	F932	-6.4 ± 0.8	-8.1 ± 0.9	-5.7 ± 1.0
SGF29	F264	-0.8 ± 0.3	-3.4 ± 1.0	-2.1 ± 0.7
	Y238	-3.5 ± 0.8	-10.2 ± 1.9	-8.3 ± 1.4
	Y245	-7.7 ± 1.0	-10.2 ± 1.8	-7.0 ± 1.5
TAF3	W868	-9.7 ± 3.4	-12.6 ± 1.7	-7.2 ± 2.3
	W891	-8.8 ± 4.3	-13.8 ± 0.9	-8.2 ± 2.4

6. Quantum chemical analyses

6.1 General Procedure

All calculations were carried out with the Amsterdam Density Functional (ADF) program using dispersion-corrected density functional theory at the BLYP-D3BJ/TZ2P level of theory.[11,12] The effect of solvation was simulated by means of the Conductor like Screening Model (COSMO) of solvation as implemented in ADF. The approach has been benchmarked against highly correlated post-Hartree-Fock methods and experimental data and was found to work reliably.[13-15]

6.2 Bonding Analysis

The bonding mechanism in our model complexes have been further analysed using quantitative (Kohn-Sham) molecular orbital (MO) theory in combination with an energy decomposition analysis (EDA).[16,17] The bond energy in aqueous solution ΔE(aq) consists of two major components, namely, the strain energy ΔE_{strain}(aq) associated with deforming the KMe3 and the reader from their own equilibrium structure to the geometry they adopt in the complex, plus the interaction energy ΔE_{int}(aq) between these deformed solutes in the complex (see Eq. 1):

$$\Delta E(\text{aq}) = \Delta E_{strain}(\text{aq}) + \Delta E_{int}(\text{aq}). \quad (1)$$

To arrive at an understanding of the importance of desolvation phenomena during the complexation process, we separate the solute–solute interaction ΔE_{int}(aq) into the effect caused by the change in solvation ΔE(desolv) and the remaining intrinsic interaction ΔE_{int} between the unsolvated fragments in vacuum ΔE_{int}:

$$\Delta E_{int}(\text{aq}) = \Delta E_{int}(\text{desolv}) + \Delta E_{int}. \quad (2)$$

In the EDA, the intrinsic interaction energy ΔE_{int} can be further decomposed as shown in Eq. 3:

$$\Delta E_{int} = \Delta V_{elstat} + \Delta E_{Pauli} + \Delta E_{oi} + \Delta E_{disp}. \quad (3)$$

Here, ΔV_{elstat} corresponds to the classical electrostatic interaction between the unperturbed charge distributions of the deformed fragments which is usually attractive. The Pauli repulsion ΔE_{Pauli} comprises the destabilizing interactions between occupied orbitals and is responsible for the steric repulsions. The orbital interaction ΔE_{oi} accounts for charge transfer (donor–acceptor interactions between occupied orbitals on one moiety with unoccupied orbitals of the other, including the HOMO–LUMO interactions) and polarization (empty/occupied orbital mixing on

one fragment due to the presence of another fragment). Finally, the ΔE_{disp} term accounts for the dispersion interactions based on Grimme's DFT-D3BJ correction. Furthermore, the charge distribution has been analysed using the Voronoi deformation density (VDD) method.[18]

6.3 Geometry optimization

TRP2-KMe3 was terminated with one hydrogen at C_β of the KMe3 side chain and one hydrogen at each C_β of the TRP2 fragment. For OrnMe3 and hKMe3, we have used the same X-ray structure as for KMe3, however, with one CH_2 less in the former and one CH_2 more in the latter. To simulate the structural rigidity that is imposed by the protein backbone in the full protein system, the TRP2 fragment is kept frozen to the X-ray structure, both as a separate fragment and in the complexes. The KMe3 fragment is fully optimized, not only as isolated molecule but also as molecular fragment in its complex with TRP2. The OrnMe3 and hKMe3 fragments are also fully optimized as isolated molecules; but in the complex with TRP2, the carbon of the alpha methyl group is kept constrained at the same position with respect to TRP2 as in the TRP2-KMe3. The latter constraint simulates that, in the real complex, the remainder of OrnMe3 and hKMe3, which is not present in our simple model, is kept at its position relative to KDM5A through intermolecular interactions in the same way as KMe3. Geometry of the optimized KMe3 model system differs only very slightly from the X-ray structure.

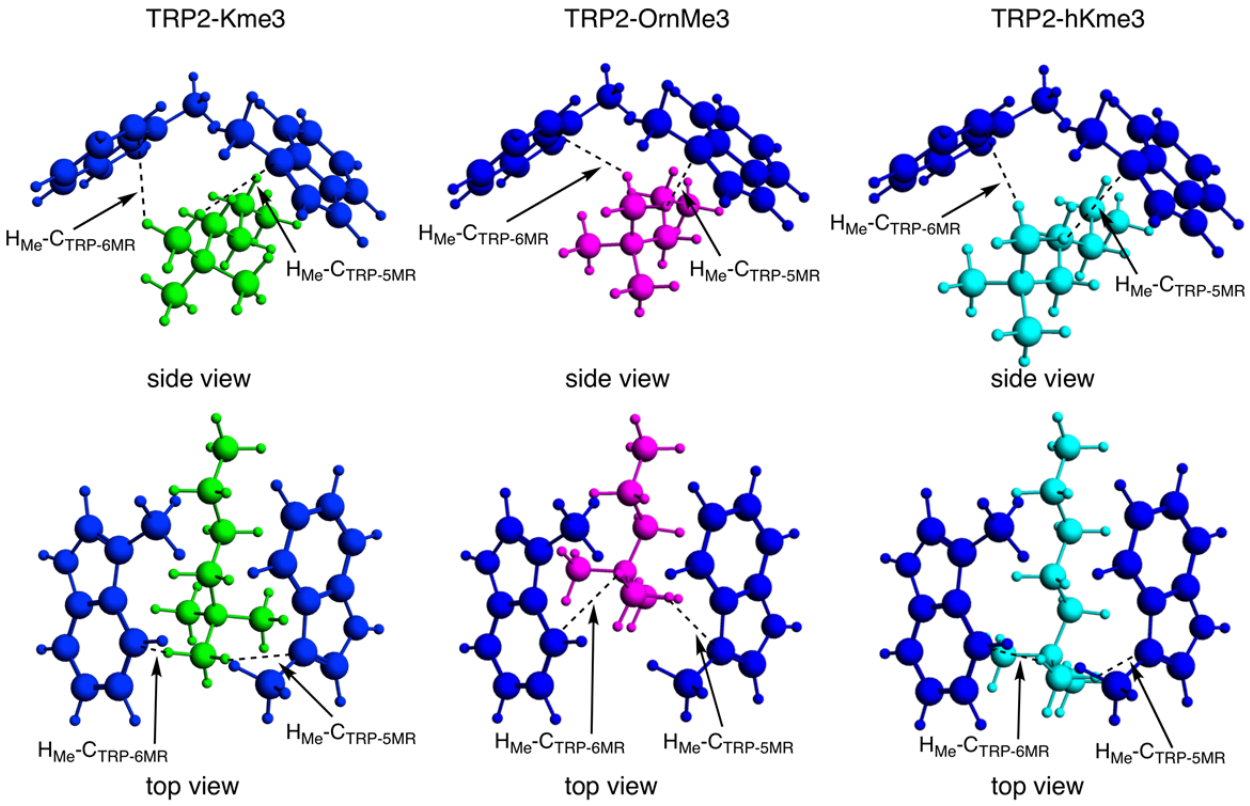

Fig. S31 Structure of TRP2-KMe3, TRP2-OrnMe3 and TRP2-hKMe3 model complexes: TRP2 in blue, KMe3 in green, OrnMe3 in pink, and hKMe3 in turquoise.

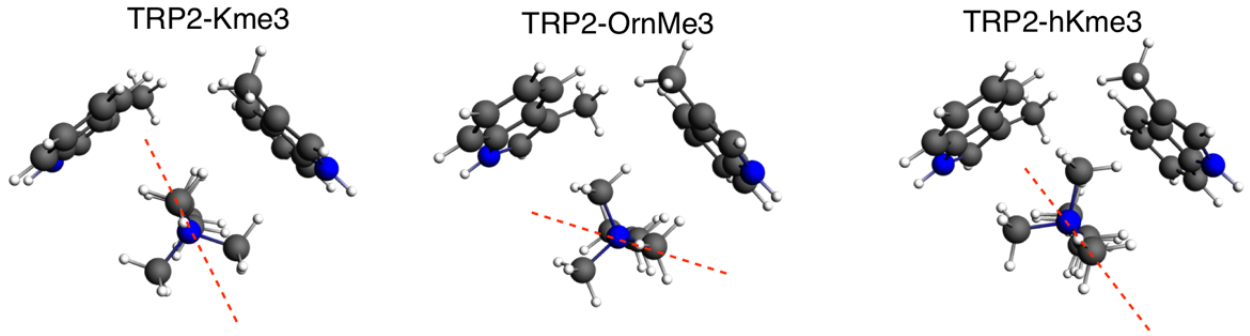

Fig. S32 Front view of the structure of TRP2-KMe3, TRP2-OrnMe3 and TRP2-hKMe3 model complexes. The plane that encloses the chain from NMe_3^+ till C_α in red.

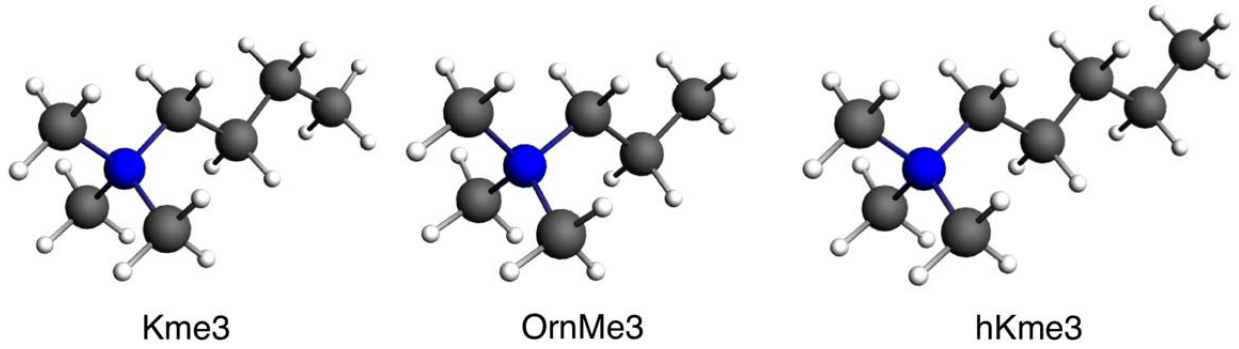

Fig. S33 Relaxed KMe3, OrnMe3 and hKMe3 at COSMO-BLYP-D3BJ/TZ2P level.

Table S5 Overlaps between the MOs of TRP2 and KMe3, OrnMe3, or hKMe3.[a]

TRP2 MOs	**KMe3/OrnMe3/hKMe3 MOs**	**TRP2-KMe3**	**TRP2-OrnMe3**	**TRÑ2-hKMe3**
HOMO	LUMO	0.012	0.003	0.020
HOMO	LUMO+1	0.006	0.007	0.002
HOMO-1	**LUMO**	**0.028**	**0.012**	**0.025**
HOMO-1	LUMO+1	0.006	0.008	0.007

[a] Computed at BLYP-D3BJ/TZ2P.

Table S6 Cartesian coordinates (in Å) of TRP2-KMe3, TRP2-OrnMe3 and TRP2-hKMe3 complexes, computed at BLYP-D3BJ/TZ2P using COSMO to simulate aqueous solvation and a constrained optimization to simulate the effect of the protein backbone.

TRP2-KMe3:

C	-14.114000000	-20.049000000	-0.875000000
C	-14.962000000	-19.738000000	0.323000000
C	-15.235000000	-20.561000000	1.377000000
C	-15.571000000	-18.476000000	0.628000000
C	-16.191000000	-18.610000000	1.893000000
C	-15.649000000	-17.250000000	-0.044000000
N	-15.971000000	-19.886000000	2.326000000
C	-16.882000000	-17.550000000	2.500000000
C	-16.335000000	-16.198000000	0.561000000
C	-16.943000000	-16.358000000	1.823000000
H	-17.473000000	-15.517000000	2.270000000
H	-14.000000000	-19.128000000	-1.447000000
H	-14.917000000	-21.601000000	1.456000000
H	-15.183000000	-17.121000000	-1.021000000
H	-16.295000000	-20.273000000	3.201000000
H	-17.354000000	-17.669000000	3.475000000
H	-16.402000000	-15.237000000	0.051000000
H	-13.186000000	-20.452000000	-0.470000000
C	-13.008000000	-14.944000000	-1.752000000
C	-11.604000000	-15.279000000	-1.421000000
C	-10.629000000	-14.423000000	-0.994000000
C	-10.999000000	-16.571000000	-1.507000000
C	-9.651000000	-16.428000000	-1.114000000
C	-11.469000000	-17.840000000	-1.880000000
N	-9.451000000	-15.109000000	-0.805000000
C	-8.764000000	-17.507000000	-1.084000000
C	-10.588000000	-18.912000000	-1.851000000
C	-9.247000000	-18.738000000	-1.453000000
H	-8.579000000	-19.599000000	-1.438000000
H	-13.651000000	-15.747000000	-1.391000000
H	-10.764000000	-13.354000000	-0.828000000
H	-12.506000000	-17.981000000	-2.186000000
H	-8.581000000	-14.705000000	-0.490000000
H	-7.726000000	-17.376000000	-0.779000000
H	-10.938000000	-19.903000000	-2.140000000
H	-13.236000000	-13.992000000	-1.272000000
H	-14.522374582	-20.815706247	-1.547885097
H	-13.158423449	-14.818069475	-2.834003080
C	-10.114752602	-21.305220763	1.892377384
C	-11.216790553	-20.285805453	1.565697139

C	-11.002507694	-18.940388922	2.287874794
C	-12.090102444	-17.946438531	1.883398917
N	-12.070579136	-16.609009105	2.645799587
C	-13.150209827	-15.721875154	2.061139245
C	-10.731973677	-15.916856909	2.492497579
C	-12.365551231	-16.823749860	4.115733524
H	-12.408951734	-15.846708144	4.598931529
H	-9.130774938	-20.927740553	1.584711029
H	-12.198761989	-20.691389652	1.844793551
H	-10.013332154	-18.548608026	2.021388165
H	-13.089556823	-18.360771942	2.048366284
H	-12.918787327	-15.550085307	1.009793743
H	-10.798479096	-14.941374934	2.976931329
H	-11.570405162	-17.423783848	4.555007649
H	-10.074709060	-21.512398227	2.969877086
H	-11.238229637	-20.105747697	0.484787617
H	-11.011890000	-19.111207919	3.371339633
H	-11.995495315	-17.683123359	0.825941434
H	-13.153012338	-14.778635478	2.609325685
H	-10.522561113	-15.800602201	1.428638506
H	-13.326128627	-17.334212341	4.203429545
H	-14.111323996	-16.226695834	2.162298263
H	-9.963428736	-16.520728269	2.972373589
H	-10.290718944	-22.253949886	1.371226478

TRP2-OrnMe3:

C	-14.114000	-20.049000	-0.875000
C	-14.962000	-19.738000	0.323000
C	-15.235000	-20.561000	1.377000
C	-15.571000	-18.476000	0.628000
C	-16.191000	-18.610000	1.893000
C	-15.649000	-17.250000	-0.044000
N	-15.971000	-19.886000	2.326000
C	-16.882000	-17.550000	2.500000
C	-16.335000	-16.198000	0.561000
C	-16.943000	-16.358000	1.823000
H	-17.473000	-15.517000	2.270000
H	-14.000000	-19.128000	-1.447000
H	-14.917000	-21.601000	1.456000
H	-15.183000	-17.121000	-1.021000
H	-16.295000	-20.273000	3.201000
H	-17.354000	-17.669000	3.475000
H	-16.402000	-15.237000	0.051000
H	-13.186000	-20.452000	-0.470000
C	-13.008000	-14.944000	-1.752000

C	-11.604000	-15.279000	-1.421000
C	-10.629000	-14.423000	-0.994000
C	-10.999000	-16.571000	-1.507000
C	-9.651000	-16.428000	-1.114000
C	-11.469000	-17.840000	-1.880000
N	-9.451000	-15.109000	-0.805000
C	-8.764000	-17.507000	-1.084000
C	-10.588000	-18.912000	-1.851000
C	-9.247000	-18.738000	-1.453000
H	-8.579000	-19.599000	-1.438000
H	-13.651000	-15.747000	-1.391000
H	-10.764000	-13.354000	-0.828000
H	-12.506000	-17.981000	-2.186000
H	-8.581000	-14.705000	-0.490000
H	-7.726000	-17.376000	-0.779000
H	-10.938000	-19.903000	-2.140000
H	-13.236000	-13.992000	-1.272000
H	-14.522375	-20.815706	-1.547885
H	-13.158423	-14.818069	-2.834003
C	-10.114753	-21.305221	1.892377
C	-11.153599	-20.218854	2.240584
C	-10.502512	-18.835450	2.176074
H	-10.578052	-22.296792	1.926202
N	-11.398649	-17.660382	2.608559
C	-12.636680	-17.582076	1.741891
C	-10.602808	-16.380419	2.448897
C	-11.810607	-17.798035	4.059702
H	-12.378185	-16.908165	4.335537
H	-9.707445	-21.151859	0.885349
H	-11.550996	-20.412053	3.243004
H	-10.184826	-18.603511	1.154509
H	-9.713132	-16.447431	3.075782
H	-12.324018	-17.507112	0.698915
H	-11.229751	-15.546432	2.766755
H	-10.909713	-17.878650	4.669679
H	-9.280291	-21.292150	2.604015
H	-11.992536	-20.276221	1.537972
H	-9.629191	-18.787046	2.833811
H	-13.233647	-18.478703	1.896403
H	-13.205941	-16.698364	2.034867
H	-10.326458	-16.272834	1.399969
H	-12.430284	-18.686585	4.172481

TRP2-hKMe3:

C	-14.114000	-20.049000	-0.875000
C	-14.962000	-19.738000	0.323000
C	-15.235000	-20.561000	1.377000
C	-15.571000	-18.476000	0.628000
C	-16.191000	-18.610000	1.893000
C	-15.649000	-17.250000	-0.044000
N	-15.971000	-19.886000	2.326000
C	-16.882000	-17.550000	2.500000
C	-16.335000	-16.198000	0.561000
C	-16.943000	-16.358000	1.823000
H	-17.473000	-15.517000	2.270000
H	-14.000000	-19.128000	-1.447000
H	-14.917000	-21.601000	1.456000
H	-15.183000	-17.121000	-1.021000
H	-16.295000	-20.273000	3.201000
H	-17.354000	-17.669000	3.475000
H	-16.402000	-15.237000	0.051000
H	-13.186000	-20.452000	-0.470000
C	-13.008000	-14.944000	-1.752000
C	-11.604000	-15.279000	-1.421000
C	-10.629000	-14.423000	-0.994000
C	-10.999000	-16.571000	-1.507000
C	-9.651000	-16.428000	-1.114000
C	-11.469000	-17.840000	-1.880000
N	-9.451000	-15.109000	-0.805000
C	-8.764000	-17.507000	-1.084000
C	-10.588000	-18.912000	-1.851000
C	-9.247000	-18.738000	-1.453000
H	-8.579000	-19.599000	-1.438000
H	-13.651000	-15.747000	-1.391000
H	-10.764000	-13.354000	-0.828000
H	-12.506000	-17.981000	-2.186000
H	-8.581000	-14.705000	-0.490000
H	-7.726000	-17.376000	-0.779000
H	-10.938000	-19.903000	-2.140000
H	-13.236000	-13.992000	-1.272000
H	-14.522375	-20.815706	-1.547885
H	-13.158423	-14.818069	-2.834003
C	-10.114753	-21.305221	1.892377
C	-11.202222	-20.247461	1.649195
C	-10.848955	-18.889995	2.275142
C	-11.983281	-17.854090	2.144786
C	-11.567251	-16.568228	2.856028
N	-12.666734	-15.506907	3.026409

H	-11.221005	-16.781920	3.871553
H	-10.381195	-22.266063	1.434551
H	-12.186203	-17.664522	1.084664
H	-9.155408	-20.983963	1.464419
H	-12.160738	-20.596359	2.059452
H	-9.938558	-18.497499	1.798833
H	-12.895701	-18.270664	2.587563
H	-13.701550	-15.920259	1.212413
H	-11.239563	-13.929435	3.097285
H	-13.388108	-16.389958	4.824499
H	-9.961900	-21.473661	2.966968
H	-11.348947	-20.109970	0.571326
H	-10.616375	-19.032543	3.341647
H	-10.759801	-16.068701	2.311790
C	-13.802059	-16.036225	3.879041
H	-14.502691	-15.218381	4.053039
H	-14.303458	-16.843686	3.346923
C	-12.049978	-14.309340	3.720368
H	-12.822019	-13.549843	3.848274
H	-11.667443	-14.630803	4.689425
C	-13.201642	-15.074498	1.681373
H	-13.915477	-14.264861	1.840976
H	-12.363160	-14.738304	1.069794

7. References

1. A. H. K. Al Temimi, Y. V. Reddy, P. B. White, H. Guo, P. Qian and J. Mecinović, *Sci. Rep.*, 2017, **7**, 16148.
2. R. Belle, A. H. K. Al Temimi, K. Kumar, B. J. G. E. Pieters, A. Tumber, J. E. Dunford, C. Johansson, U. Oppermann, T. Brown, C. J. Schofield, R. J. Hopkinson, R. S. Paton, A. Kawamura and J. Mecinović, *Chem. Commun.*, 2017, **53**, 13264-13267.
3. J. J. A. G. Kamps, J. Huang, J. Poater, C. Xu, B. J. G. E. Pieters, A. Dong, J. Min, W. Sherman, T. Beuming, F. M. Bickelhaupt, H. Li and J. Mecinović, *Nat. Commun.,* 2015, **6**, 8911.
4. D. A. Case, T. A. Darden, T. E. Cheatham, C. L. Simmerling, J. Wang, R. E. Duke, R. Luo, R. C. Walker, W. Zhang, K. M. Merz, B. Roberts, S. Hayik, A. Roitberg, G. Seabra, J. Swails, A. W. Götz, I. Kolossváry, K. F. Wong, F. Paesani, J. Vanicek, R. M. Wolf, J. Liu, X. Wu, S. R. Brozell, T. Steinbrecher, H. Gohlke, Q. Cai, X. Ye, J. Wang, M.-J. Hsieh, G. Cui, D. R. Roe, D. H. Mathews, M. G. Seetin, R. Salomon-Ferrer, C. Sagui, V. Babin, T. Luchko, S. Gusarov, A. Kovalenko and P. A. Kollman, *AMBER 12, University of California, San Francisco*, 2012.
5. W. L. Jorgensen, J. Chandrasekhar, J. D. Madura, R. W. Impey and M. L. Klein, *J. Chem. Phys.*, 1983, **79**, 926–935.
6. W. A. Cortopassi, R. Simion, C. E. Honsby, T. C. C. França and R. S. Paton, *Chem. - A Eur. J.*, 2015, **21**, 18983–18992.
7. W. A. Cortopassi, K. Kumar, R. S. Paton, E. Komives, W. Wang, S. Müller, S. Knapp, F. Bracher, L. Kale, K. Schulten, D. F. Ortwine, T. Lu, Y. D. Chen, C. Yapp, P. Filippakopoulos, M. E. Bunnage, S. Muller, S. Knapp, C. J. Schofield, P. E. Brennan, D. Lugo, P. Jeffrey, S. Taylor, M. L. Vecellio, C. Bountra, P. E. Brennan, A. O'Mahony, S. Velichko, S. Muller, D. Hay, D. L. Daniels, M. Urh, N. B. La Thangue, T. Kouzarides, R. Prinjha, J. Schwaller and S. Knapp, *Org. Biomol. Chem.*, 2016, **14**, 10926–10938.
8. C. I. Bayly, P. Cieplak, W. Cornell and P. A. Kollman, *J. Phys. Chem.*, 1993, **97**, 10269–10280.
9. H. Wang, F. Dommert and C. Holm, *J. Chem. Phys.*, 2010, **133**, 34117.
10. J. C. Phillips, R. Braun, W. Wang, J. Gumbart, E. Tajkhorshid, E. Villa, C. Chipot, R. D. Skeel, L. Kalé and K. Schulten, *J. Comput. Chem.*, 2005, **26**, 1781–1802.
11. G. Te Velde *et al.*, *J. Comput. Chem.*, 2011, **22,** 931–967.
12. A. D. Becke, *Phys. Rev. A*, 1988, **38,** 3098–3100.
13. C. Fonseca Guerra, T. van der Wijst, J. Poater, M. Swart and F. M. Bickelhaupt, *Theor. Chem. Acc.*, 2010, **125**, 245–252.
14. T. Van der Wijst, C. Fonseca Guerra, M. Swart, F. M. Bickelhaupt and B. A. Lippert, *Angew. Chem. Int. Ed.,* 2009, **48**, 3285–3287.
15. J. Simo Padial, R. de Gelder, C. Fonseca Guerra, F. M. Bickelhaupt and J. Mecinović, *Chem. Eur. J.,* 2014, **20**, 6268–6271.
16. F. M. Bickelhaupt and E. J. Baerends, in *Reviews in Computational Chemistry,* 2000, **15**, 1–86 (Wiley, Weilheim).
17. E. J. Baerends, O. V. Gritsenko and R. van Meer, *Phys. Chem. Chem. Phys.,* 2013, **15**, 16408-16425
18. C. Fonseca Guerra, J. W. Handgraaf, E. J. Baerends and F. M. Bickelhaupt, *J. Comput. Chem.,* 2004, **25,** 189–210.